View metadata, citation and similar papers at core.ac.uk
brought to you by CORE
provided by RERO DOC Digital Library

Geophys. J. Int. (1998) 135, 195–214

Crustal strain in central Greece from repeated GPS measurements in the interval 1989–1997

P. J. Clarke,[1] R. R. Davies,[1,*] P. C. England,[1] B. Parsons,[1] H. Billiris,[2] D. Paradissis,[2] G. Veis,[2] P. A. Cross,[3,†] P. H. Denys,[3,§] V. Ashkenazi,[4] R. Bingley,[4] H.-G. Kahle,[5] M.-V. Muller[5] and P. Briole[6]

[1] *Department of Earth Sciences, University of Oxford, Parks Road, Oxford,* OX1 3PR, *UK. E-mail: peter.clarke@earth.ox.ac.uk*
[2] *Higher Geodesy Laboratory, National Technical University of Athens,* 15780 *Zographos, Athens, Greece*
[3] *Department of Geomatics, University of Newcastle upon Tyne, Newcastle,* NE1 7RU, *UK*
[4] *Institute of Engineering Surveying and Space Geodesy, University of Nottingham, Nottingham,* NG7 2RD, *UK*
[5] *Institut für Geodäsie und Photogrammetrie, ETH Hönggerberg,* CH-8093 *Zürich, Switzerland*
[6] *Institut de Physique du Globe,* 4 *Place Jussieu,* 75252 *Paris Cedex* 05, *France*

Accepted 1998 May 8. Received 1998 May 8; in original form 1997 September 8

SUMMARY

A 66-station GPS network spanning central Greece, first observed in 1989, has been occupied fully on three occasions: June 1989, October 1991 and May 1993. Subsets of this network bounding the Gulf of Korinthos have also been occupied in June 1995, October 1995, May 1996 and September/October 1997. The first three occupations were processed using a fiducial GPS methodology, whereas later surveys were processed using CODE precise orbits. Combination of data from different surveys to yield smooth site velocities requires global network translations at each epoch to compensate for errors in the realization of the reference frame. This method provides *a posteriori* estimates of the relative coordinate errors and reference frame noise. Only one earthquake, the 1995 June 15 Egion event, has caused significant local coseismic displacement, and its effects on the interseismic velocity field are removed using an elastic dislocation model.

We constrain the orientation of the 100 yr triangulation–GPS velocity estimates of Davies *et al.* (1997) using 14 sites common to the two networks. The goodness of fit of this transformation indicates that the short-term and 100 yr geodetic estimates of deformation are highly compatible. We infer that short-term geodetic studies are capable of determining longer-term deformation rates provided that transient, local effects can be modelled. From the combined velocity field, we estimate principal strains and rigid-body rotation rates at points on a regular grid using data from neighbouring sites. Strain rates are high within the Gulf of Korinthos and much lower elsewhere. The extension rate across the Gulf of Korinthos increases from east to west. Comparison of the extension rate with historical and recent rates of seismic release of strain reveals significant medium-term seismic hazard in the western Gulf of Korinthos, and may also indicate long-term aseismic strain.

Key words: GPS, Greece, seismic hazard, strain, velocity field.

INTRODUCTION

The Eastern Mediterranean is one of the most tectonically active areas on the Earth's surface (e.g. McKenzie 1972, 1978), as is demonstrated by its seismicity (Fig. 1). Deep seismicity under the Sea of Crete is related to the subduction of northward-moving (relative to Eurasia) African oceanic lithosphere, whereas shallow seismicity throughout the Aegean Sea and mainland Greece is related to the southwestward (again relative to Eurasia) extension of Aegean continental lithosphere driven by a combination of gravitational spreading of the Anatolian continental lithosphere from the east and roll-back of the subducting African plate to the south (Le Pichon & Angelier 1979). The tectonic evolution of the region has been covered extensively elsewhere (McKenzie 1972, 1978; Dewey & Şengör 1979; Le Pichon & Angelier

* Now at: Research School of Earth Sciences, Victoria University of Wellington, New Zealand.
† Now at: Department of Geomatics, University College London, Gower Street, London, WC1E 6BT, UK.
§ Now at: Department of Surveying, University of Otago, New Zealand.

© 1998 RAS

GJI000 14/9/98 12:30:03 3B2 version 5.20
The Charlesworth Group, Huddersfield 01484 517077

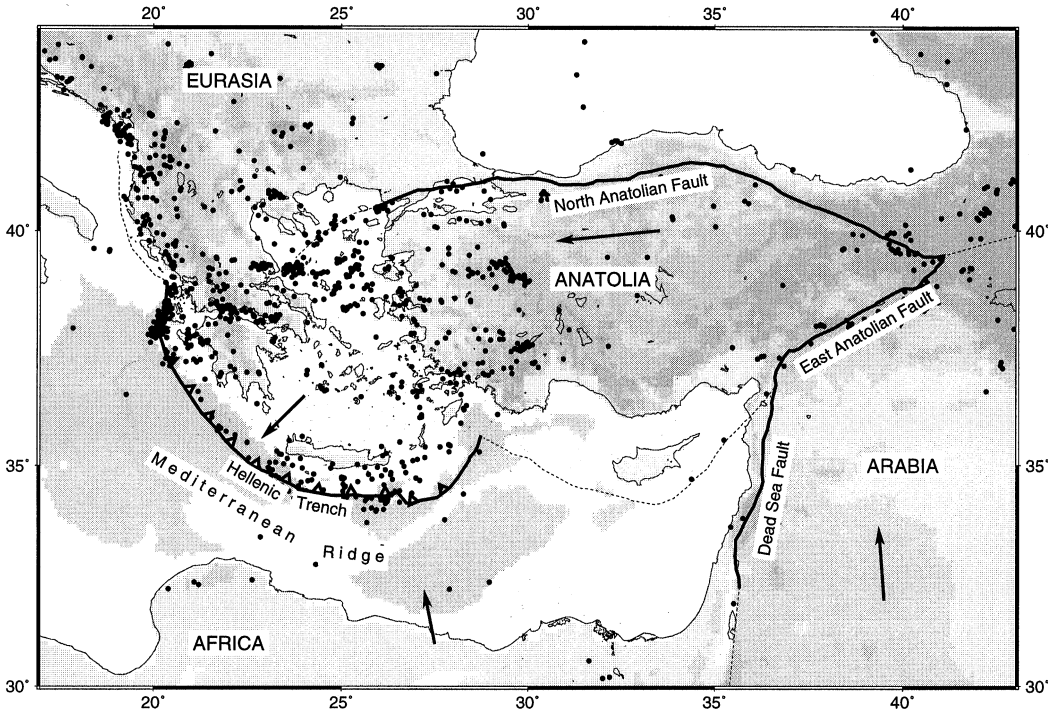

Figure 1. Large-scale tectonic features of the Eastern Mediterranean. Arrows show approximate plate motions relative to stable Eurasia. Shallow (<40 km) earthquakes of magnitude $M_b > 4.5$ from the ISC catalogue 1964–1993 are shown as dots. Topographic shading increases at 500 m vertical intervals, and in addition seafloor below 2500 m depth is shaded.

1981; Angelier *et al*. 1982; Armijo *et al.* 1996) and so is not elaborated upon here; the purpose of this paper is to present recent space-geodetic data that constrain current deformation rates in central Greece, and compare them with longer-term geodetic data.

Crustal movement within the Aegean region is accommodated on a large number of known faults, and probably also many unmapped ones. Because these faults encompass a wide variety of orientations, geometries and faulting styles, the deformation of the zone at length-scales much larger than a single fault is best described as a continuum (Jackson & McKenzie 1988b). Subregions within the zone probably deform at least partially aseismically, for example the Hellenic Trench (Jackson & McKenzie 1988a), and some show no seismic expression of strain, for example the Sea of Crete. At smaller length-scales, opinion is divided as to whether the deformation is best described by floating-block or slat models involving large arrays of faults (Taymaz, Jackson & McKenzie 1991) or whether it is concentrated on a few narrow, more intensely deforming zones, for example the Gulf of Korinthos (Armijo *et al.* 1996). For this reason, and because the 30-year period since the inception of the World-Wide Standardised Seismic Network (WWSSN) may be too short to characterize the seismicity within small subregions (Jackson & McKenzie 1988a; Jackson, Haines & Holt 1992; Ambraseys & Jackson 1997), geodetic measurements provide an essential complementary method of quantifying the deformation. This approach also has the advantage that it is possible to make estimates of regional medium-term seismic hazard based on the difference between geodetic deformation and that predicted from the seismic release of strain using the method of Kostrov (1974).

Previous geodetic work in the Aegean was initially conducted on a large spatial scale or over long timescales. Satellite Laser Ranging (SLR) measurements have been made at six sites within the Aegean region since 1986 (Noomen, Ambrosius & Wakker 1993; Robbins, Smith & Ma 1993). Jackson, Haines & Holt (1994) compared the SLR site velocities with those expected from seismic strain release in the period 1911–1992, and concluded that seismicity can account for at most 50 per cent of the deformation in the Aegean, although the effects of additional uncatalogued smaller earthquakes may account for some of the discrepancy. Other workers (Kastens *et al.* 1989; Gilbert *et al.* 1994; R. Reilinger, personal communication, 1998) have obtained velocity estimates at similar length-scales in the Aegean region using GPS data from 1988–1996.

At a smaller scale, Billiris *et al.* (1991) and Davies *et al.* (1997) have reanalysed 100-year-old triangulation data from southern and central Greece and compared them with data from a partial reoccupation of the original network using the Global Positioning System (GPS). These data span a much longer timescale than can purely space-geodetic experiments, and thus sample a larger deformational signal, but this advantage is counteracted by the lower precision of triangulation measurements (roughly 3 ppm compared to 0.05 ppm for GPS). Even at this scale of observation Davies *et al.* (1997) were able to distinguish zones with very little deformation (for example the central Peloponnesos) from zones with far higher deformation (for example the Gulf of Korinthos).

The advantages of modern GPS–GPS velocity field determinations over triangulation–GPS methods are (1) that there is no longer a need to make scale and orientation assumptions to generate a unique velocity field, (2) the network can be designed with geodynamic studies in mind rather than station

GJI000 14/9/98 12:30:42 3B2 version 5.20
The Charlesworth Group, Huddersfield 01484 517077

intervisibility requirements, and (3) stations can be sited more densely than the old first-order triangulation pillars. Kahle and colleagues (Kahle *et al.* 1993, 1995; Kahle, Muller & Veis 1996) have occupied sites from a 46-station GPS network in western Greece, the Ionian Sea and Crete up to four times over the period 1989–1994. They conclude that the northeastward subduction of the Mediterranean seafloor is taken up along the Kephalonia Fault Zone in the Ionian Sea. This network abuts the western side of the Central Greece Network; seven sites (including three SLR sites) are common to both experiments. Agatza-Balodmou *et al.* (1995) have also reported some initial results from a GPS network spanning the Gulf of Korinthos, which has some sites in common with the Central Greece Network.

The Central Greece Network (CGN) was established in 1988 for the purpose of studying present-day crustal motions in the region surrounding the gulfs of Korinthos and Evvia (Fig. 2). The majority of site markers take the form of brass pins glued into (usually limestone) bedrock. In addition to the primary mark, two or three witness marks were installed at each site to permit reconstruction of the primary in the event of damage. Local site ties have been determined by optical surveying. Three sites (54, Dionysos, DION; 16, Xrisokellaria, XRIS; 18, Karitsa, KRTS) form part of the WEGENER/MEDLAS network and have also been occupied with SLR at various times since 1986 (Noomen *et al.* 1993; Robbins *et al.* 1993). Seven stations (11, 13, 21, 44, 48, 49, 59) are concrete triangulation pillars forming part of the Hellenic Army Geographic Service (HAGS) network; of these, sites 44, 48 and 59 correspond to sites VALT, MKPG and CLMU of the 1890s first-order triangulation network (Billiris *et al.* 1991; Davies *et al.* 1997), and sites 11 and 21 are eccentric pillars of the 1890s sites SKOP and KNIM.

GPS OBSERVATIONS

The CGN has been occupied fully three times: in June 1989, October 1991 and May 1993. In addition, several stations around the Gulf of Korinthos were occupied immediately after the 1995 June 15 Egion earthquake, and again in October 1995 and May 1996. A further subset of the network, predominantly those sites surrounding the Gulf of Evvia, was occupied during two successive campaigns in September and October 1997. All campaigns were referenced to the GPS/SLR site at DION. In 1989, a mixture of single-frequency and dual-frequency receivers was used; in later epochs dual-frequency receivers were used throughout. CGN sites are spaced 10–20 km apart, and daily networks were designed to include a range of processed baseline lengths to aid integer ambiguity resolution. The variety of observing strategies described below reflects the various constraints encountered at each survey epoch.

In June 1989, six dual-frequency receivers (four Leica WM102, two Trimble 4000SLD) and six single-frequency receivers (two Leica WM101, two Trimble 4000SL, two Trimble 4000SX) were used to measure the network. DION (point C) was occupied for 5 hr each day using a dual-frequency receiver.

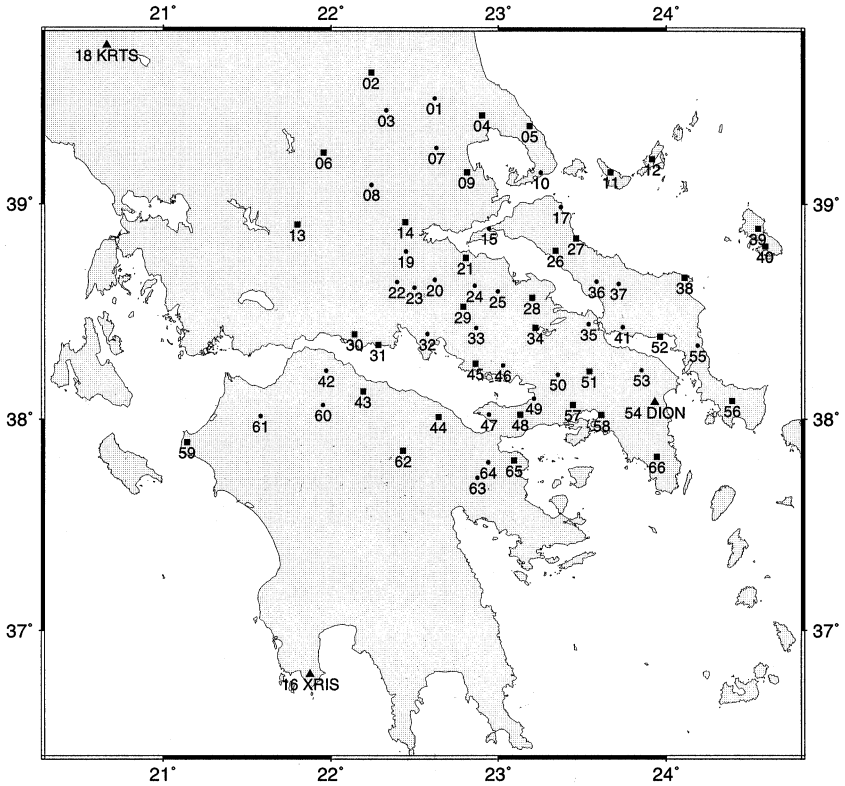

Figure 2. Sites of the Central Greece Network. Triangles indicate sites also occupied with SLR (see text). These, and sites shown as squares, were occupied with dual-frequency receivers in 1989, 1991 and 1993; other sites were occupied with dual-frequency receivers in 1991 and 1993 only. Markers bordering the Gulf of Korinthos were also occupied in 1995 and 1996 (see Fig. 3 and text), and a selection of sites mainly around the Gulf of Evvia was observed in September/October 1997 (see Fig. 4).

© 1998 RAS, *GJI* **135,** 195–214

Other sites were occupied for 5 hr sessions on two days; 36 sites had one or more sessions with dual-frequency receivers. The WM101 single-frequency data proved exceptionally unreliable and had to be discarded, leaving 60 sites. Data from International Terrestrial Reference Frame (ITRF) sites at Herstmonceaux (HERS), Onsalla (ONSA) and Wettzell (WETT) were available, but not on a 24-hour basis.

The survey of October 1991 took advantage of improvements in the satellite constellation in July–August 1991. 11 dual-frequency receivers (five Ashtech LM-XII, four Leica WM102, two Trimble 4000SST) were used to occupy CGN sites for 7 hr sessions on two days (with DION point C being occupied daily). Data from ITRF sites HERS, MADR (Madrid), ONSA and WETT were available on a nominal 24-hour basis, but still with significant outages.

In May 1993, 18 dual-frequency *P*-code receivers (10 Ashtech LM-XII2, five Leica SR299, three Trimble 4000SST) were used to observe 9 hr sessions on two days at each CGN site. DION (points A, C, D) was occupied continuously with one receiver of each type, so that single-receiver-type daily networks could be formed. Fiducial data from ITRF sites HERS, MADR, ONSA and WETT were available virtually continuously.

14 sites from the CGN (Fig. 3) and other newly established sites were occupied between five and 11 days after the 1995 June 15 Egion earthquake ($M_S = 6.2$, $M_0 = 5.1 \times 10^{18}$ N m, Harvard CMT) to provide the basis for future measurements of post-seismic strain. Observation sessions adhered to no fixed timetable; local base stations either side of the Gulf operated continuously so that short baselines could be formed radially from these sites. Each CGN site was occupied for a minimum of 4 hr, using Ashtech LM-XII2 (L2-squaring, because of Anti-Spoofing) or Z-XII (full-wavelength L2) receivers. Trimble 4000SST data from the new permanent GPS pillar at DION were available for part of the campaign.

In October 1995, points from the Egion post-seismic network, including 12 CGN sites (Fig. 3) were occupied with a total of 30 Ashtech Z-XII, Ashtech LM-XII2 and Trimble 4000SSE receivers. As in June 1995, no common session timetable was observed, but local base stations operated continuously throughout the campaign. CGN sites were occupied for a minimum of 24 hr each made up of two or three independent sessions. DION (Trimble 4000SST GPS pillar) data were available continuously during the campaign.

The post-seismic network was surveyed again in May 1996. 23 CGN sites, not all of which form part of the Egion post-seismic network, were measured during the survey (Fig. 3). 14 Ashtech Z-XII receivers were used to observe 7–24-hr sessions, with sites also in the post-seismic network being occupied two or three times. DION (point C) was also occupied continuously with an Ashtech Z-XII. Supplemental data were gathered at sites DION and XRIS during June and September 1996.

A campaign was carried out in September 1997 with the purpose of remeasuring sites throughout Greece that formed part of the first- and second-order triangulation of Greece in the 1970s. Several of these sites are in the subset of the 1890's triangulation network reoccupied with GPS in 1992 (Davies *et al.* 1997) or are within a few kilometres of monuments in the CGN (Fig. 4). In the latter case, the CGN site was occupied simultaneously with the triangulation pillar, using either a LM-XII2 or Z-XII Ashtech receiver, for a period of at least 4 hr, which was split into two or three independent sessions where this was logistically possible. In October 1997 a new dense network was established around the Gulf of Evvia, consisting of a mixture of existing CGN sites, triangulation pillars from the 1970s network and new monuments (Briole *et al.*, manuscript in preparation). Other CGN sites in the region (Fig. 4) were also occupied, using dual-frequency

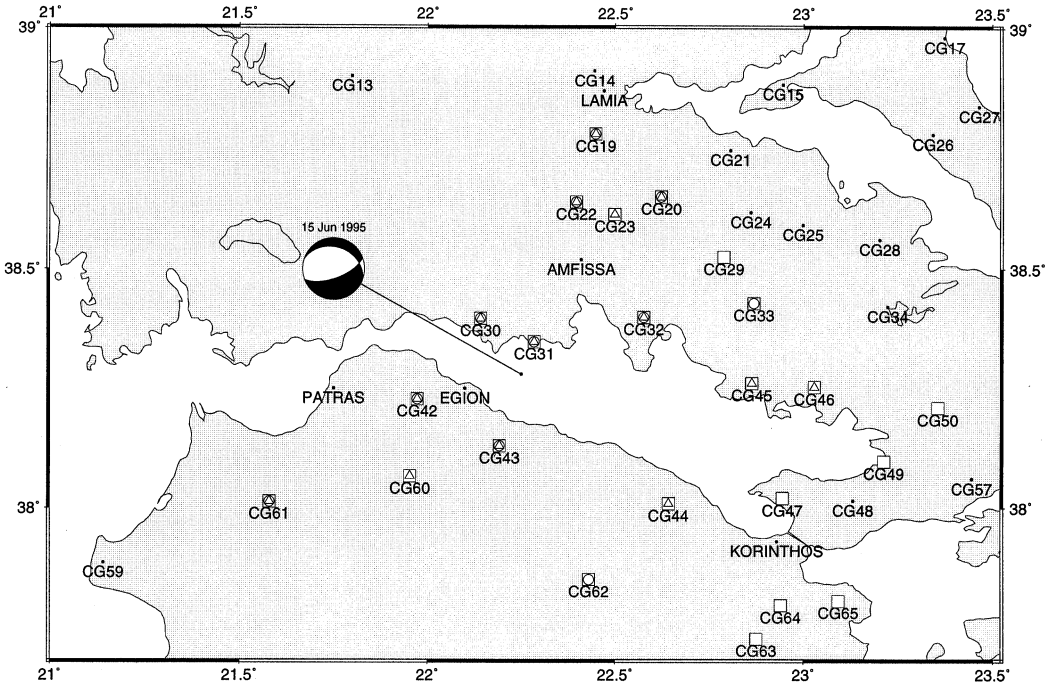

Figure 3. Location of the 1995 June 15 ($M_0 = 5.1 \times 10^{18}$ N m) Egion earthquake. Triangles denote sites occupied in June 1995, circles denote sites occupied in October 1995, and squares denote sites occupied in May 1996.

GJI000 14/9/98 12:30:58 3B2 version 5.20
The Charlesworth Group, Huddersfield 01484 517077

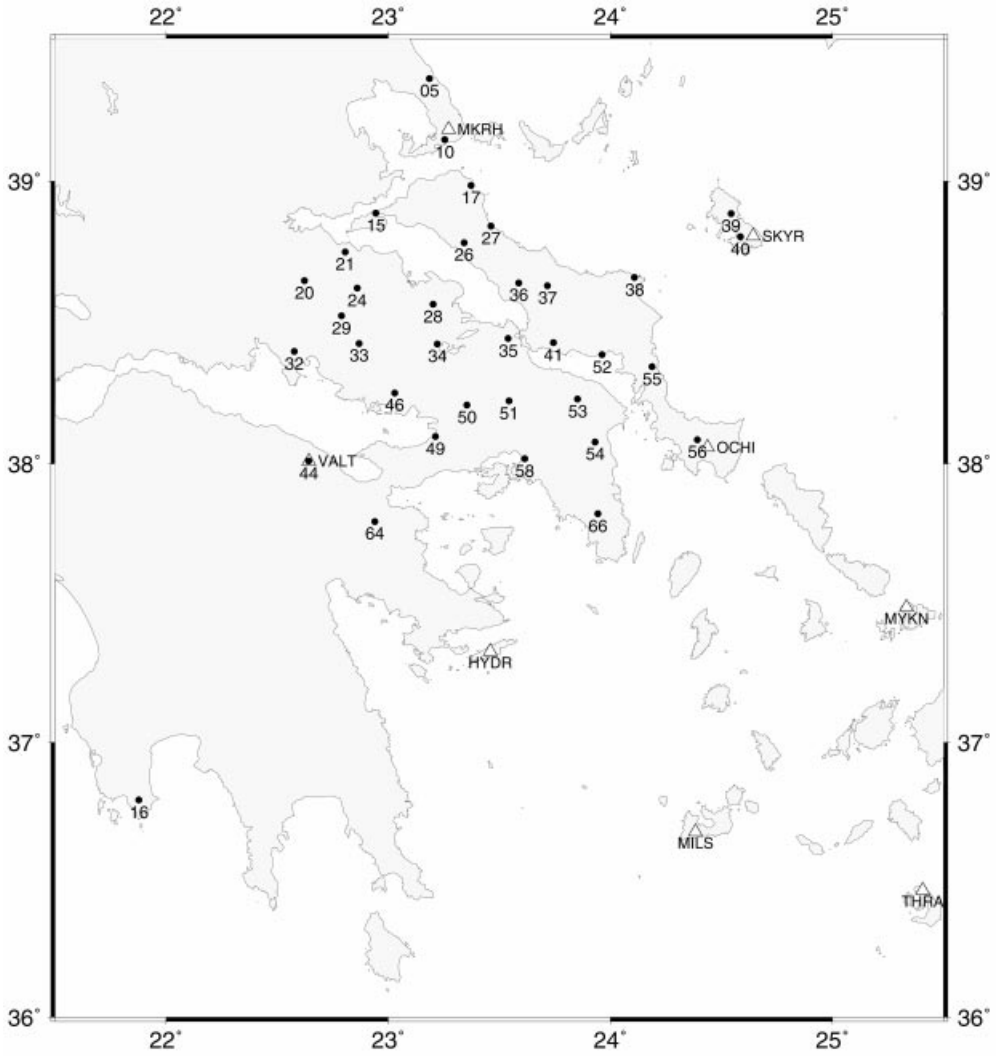

Figure 4. GPS sites in Greece reoccupied during the September and October 1997 campaigns. Triangles denote sites from the 1890s triangulation network previously occupied with GPS in 1992; circles denote CGN sites.

Ashtech and Trimble receivers, for between 6 and 120 hr in up to 11 sessions.

GPS PROCESSING

All GPS surveys have been processed at Oxford using Version 3.4 or Version 4.0 of the Bernese GPS Processing Software (Rothacher *et al.* 1993; Rothacher & Mervart 1996). The 1989, 1991 and 1993 surveys have also been processed at the University of Newcastle upon Tyne, using the same software, and at the University of Nottingham using the GAS (GPS Analysis Software) package (Stewart *et al*. 1995). Relative coordinate repeatability between different solutions at each epoch is at the level of 5 mm rms per coordinate for 1993, although it is larger for earlier surveys. Detailed comparisons of the processing methods and coordinate results are given elsewhere (Denys *et al.* 1995; University of Newcastle upon Tyne 1994); hereafter the solution referred to is that of Oxford.

All surveys were processed on a daily basis. Baselines, chosen so as to minimize length, maximize common observations, and avoid receiver- and antenna-type mixing where possible, were cleaned of cycle slips manually to ensure reliability. Carrier phase ambiguity bias parameters were fixed with typical 99 per cent success overall, except for 1991, for which an ambiguities-unresolved solution was used. Integer ambiguity fixing was achieved using wide-lane (L5) followed by ionosphere-free (L3) daily network solutions. Earlier whole-network surveys used a single-layer ionospheric Total Electron Content model to aid ambiguity fixing, whereas later Gulf of Korinthos surveys had shorter individual baselines and so did not require this. Zenith tropospheric delays at each station were estimated for 4–6 hr time windows in all network solutions. Using the ionosphere-free double-difference phase observable, final daily network coordinates were then estimated relative to DION, which was fixed at its ITRF 92 position (Boucher, Altamimi & Duhem 1993) for the survey epoch. Fully weighted coordinates were then combined using the L3D network adjustment package (Cross 1990) to produce campaign coordinate solutions; for 1989, two sets of campaign coordinates were estimated, one based on dual-frequency GPS data only, and one with all usable single- and dual-frequency

GJI000 14/9/98 12:31:10 3B2 version 5.20
The Charlesworth Group, Huddersfield 01484 517077

data. The reference frame of each coordinate set is determined by the choice of satellite orbits.

Fiducial orbits (1989, 1991, 1993)

The first three GPS surveys were processed using a fiducial GPS method (e.g. Ashkenazi *et al.* 1993) to determine precise satellite positions, because the precision available using broadcast orbits or NGS precise orbits in 1989 and 1991 was not sufficient for our purposes, and we wished to maintain a common, clearly defined reference frame between the three main survey epochs. In fiducial GPS, satellite orbits are calculated using data from sites bounding the region of interest, which are fixed to precisely known *a priori* coordinates determined by SLR, VLBI or continuous GPS measurements. To ensure internal consistency, we used the same fiducial sites (DION, HERS, MADR, ONSA, WETT) at each epoch, with the exception that MADR data were unavailable in 1989. Site coordinates were expressed in the ITRF 92 system (Boucher *et al.* 1993).

The choice of fiducial site velocity model is critical to the reference frame. All sites lie on the stable Eurasian plate except DION, which lies within the deforming region of interest. Although ITRF 92 incorporates a velocity model, for stable Eurasian sites we have used the NNR–Nuvel-1 velocity model (Argus & Gordon 1991; DeMets *et al.* 1994) because it represents in principle a more stable long-term determination of plate motions. To apply our model, we first restored the ITRF 92 positions from their quoted epoch (1988.00) to their estimated mean epoch of measurement (1992.50) using the ITRF 92 velocity model, to undo the effects of the latter, then applied the NNR–Nuvel-1 velocities. In practice, the difference between our reference frame and ITRF 92 is insignificant at the scale of the CGN for all our survey epochs, but our reference frame is in principle independent of year-to-year revisions of the ITRF velocity model that have recently occurred. Because DION lies within a deforming plate boundary zone, the NNR–Nuvel-1 plate model is inappropriate for this site, so we used the ITRF 92 velocity model only for DION.

Orbits were determined in 2- or 3-day arcs, chosen so as to minimize the effects of periods of fiducial data unavailability, using the ionosphere-free double-difference phase observable. Data from fiducial sites and dual-frequency CGN sites were used; fiducial site coordinates were held fixed and CGN site coordinates were estimated. Eight orbital parameters per satellite per arc (six osculating Keplerian elements, plus direct radiation pressure and Y-bias) were estimated, and also site zenith tropospheric delay parameters. Integer phase biases were left unresolved at this stage, so the real-valued ionosphere-free ambiguities were estimated as nuisance parameters.

Precise orbits (1995 and thereafter)

Recent improvements in precision of available post-processed orbits, especially since the GIG'92 campaign (Blewitt *et al.* 1992), allowed us to process the more recent GPS surveys using precise orbits determined elsewhere. At Oxford, we have used precise orbits from CODE (Beutler *et al.* 1994). Since 1995, these are expressed in the ITRF 93 reference frame (Boucher, Altamimi & Duhem 1994). Global rotational and scale differences between the ITRF 92 and ITRF 93 frames are of the order of a few parts per billion and so do not affect our determination of the relative positions of sites, on the scale of the CGN.

Coordinate reliability

We obtain a measure of the reliability of our coordinate estimates from the residuals of daily coordinate sets to each campaign solution (Figs 5, 6 and 7). With the exception of the 1989 survey, rms horizontal residuals are generally of the order of 10 mm per coordinate or better (15 mm rms for 1991); vertical residuals are 2–3 times higher. In 1989 the effects of short observation times, poor fiducial data quality, receiver type mixing and long baselines combine to increase the residuals to the order of 40 mm for the ionosphere-free solution (and even higher for the combined solution), so this survey adds little information to short-term crustal deformation studies. In June 1995 and May 1996, rms horizontal residuals are artificially low because most sites were only occupied once, although the session may have been split for daily network post-processing, resulting in multiple daily coordinates for a single setup. A better measure of typical day-to-day repeatability arises from the GPS occupations of the SLR sites DION, KRTS and XRIS in the 1993 campaign: each site was occupied on all 10 days of the campaign, and rms residuals at KRTS and XRIS are 10, 5, and 22 mm in the east, north and up components, respectively. We find that the formal *a posteriori* coordinate variance–covariance matrix estimated during the campaign network adjustment accurately reflects site coordinate repeatability as defined above, unlike daily coordinate variance–covariance matrix estimates from the GPS parameter inversion.

SMOOTHED VELOCITY FIELD

We use the time-series of coordinate sets obtained above to determine the *interseismic* velocities at each site; that is, the velocities that would be measured in the absence of any earthquakes. Over times that are large compared with the repeat times of large earthquakes, upper-crustal strain is accommodated, for the most part, discontinuously by slip on faults. Because of the short timescale of our geodetic observations, we are incapable of measuring directly this long-term upper-crustal strain. In the absence of large earthquakes, what is measured geodetically at the surface will reflect the long-term deformation of the underlying (lithospheric) material, irrespective of whether that deformation is continuous (e.g. Bourne, England & Parsons 1998) or discontinuous (e.g. Savage & Burford 1970). The determination of this underlying velocity field is a major reason for studying crustal velocity fields. Our measurements correspond closely to the zero-earthquake condition: only two earthquakes with $M_b \geq 5.8$ have occurred in the survey area between 1989 and 1997 (see below). As post-seismic and precursory displacements are expected to be small compared with coseismic displacements (e.g. Rundle 1982) we can obtain interseismic velocities uniformly over the region by removing the coseismic site displacements due to these large earthquakes. In addition, we must estimate the linear velocity of each site in a way that

GJI000 14/9/98 12:31:14 3B2 version 5.20
The Charlesworth Group, Huddersfield 01484 517077

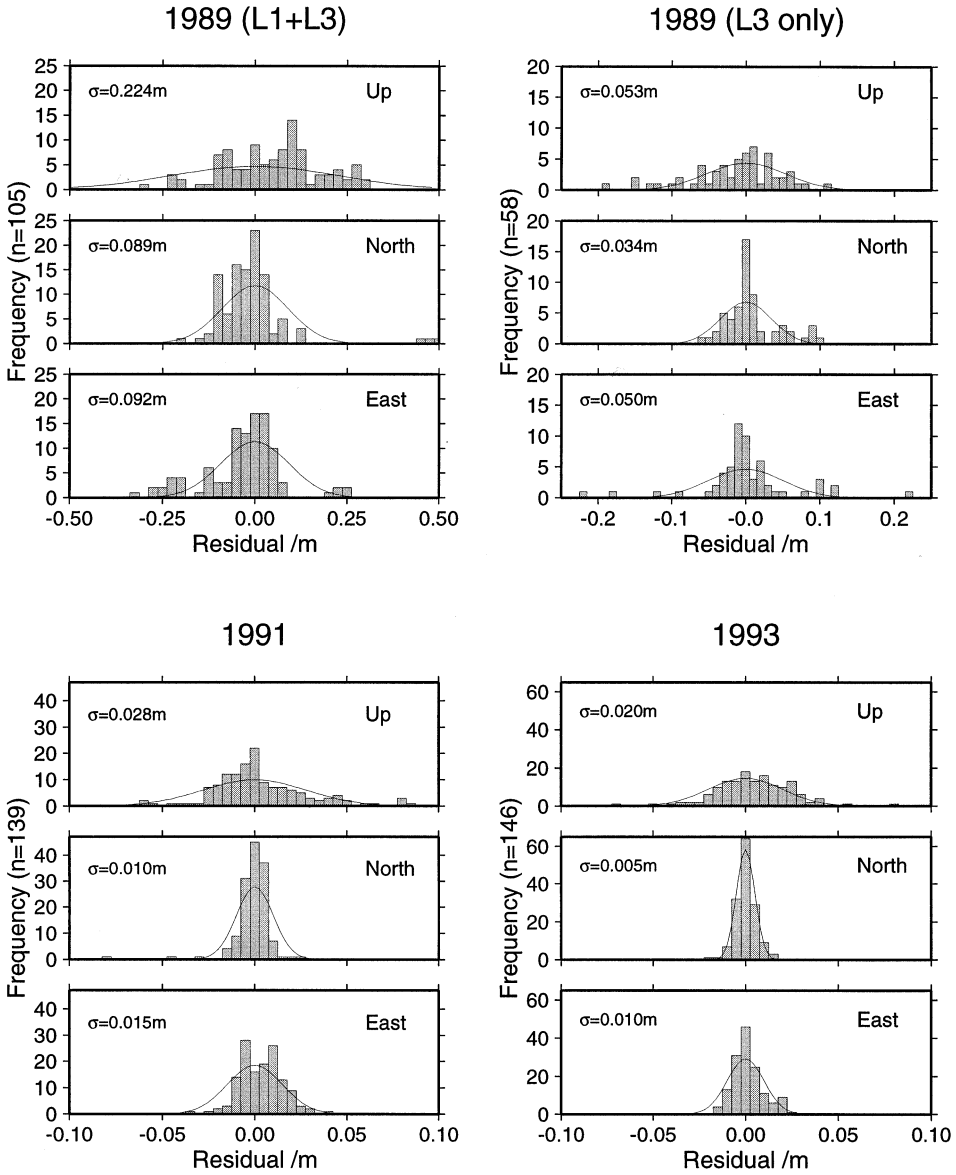

Figure 5. Residuals of daily coordinate sets to campaign solutions 1989–1993 in the local coordinate frame. Horizontal and vertical scales vary from epoch to epoch.

mitigates possible systematic errors in individual surveys. Only horizontal velocities are considered, over the interval 1989–1997.

Elimination of coseismic effects

Between 1989 and 1997, only two crustal earthquakes of magnitude $M_b \geq 5.5$ have occurred in the survey area, both in the Gulf of Korinthos. The first was the 1992 November 18 Galaxidi earthquake ($M_b = 5.8$; $M_0 = 0.85 \times 10^{18}$ N m) and the second was the 1995 June 15 Egion $M_s = 6.2$ event (and its main $M_b = 5.5$ aftershock). Coseismic displacements due to the Galaxidi earthquake, calculated using the elastic forward model of Okada (1985), are of the order of 2–3 mm, with the exception of one site (CG32), which is predicted to have been displaced by 10 mm. Even the largest displacement has marginal effect compared with the expected geodetic error over the interval 1991–1993. We therefore do not apply specific corrections for the Galaxidi earthquake or smaller events, as they will at most cause marginally significant displacements at individual sites.

In contrast, the much larger $M_0 = 5.1 \times 10^{18}$ N m Egion earthquake caused significant coseismic displacements at several sites. We have used the source model of Bernard *et al.* (1997), which is based on a combination of SAR, GPS, local seismic and teleseismic data and is independent of our data set. Bernard *et al.* (1997) propose two models: their Model A is based on both geodetic and seismological data, whereas their Model B is a better fit to the geodetic data but is inconsistent with some of the seismological and tectonic observations. Because our purpose here is to correct for geodetic coseismic displacements only, we use Model B, which best reproduces the horizontal surface movement. According to this model, sites CG30, CG31 and CG43 were displaced significantly, by amounts of the order of 40 mm; other sites have displacements of the order of 15 mm or less. We apply corrections

GJI000 14/9/98 12:31:17 3B2 version 5.20
The Charlesworth Group, Huddersfield 01484 517077

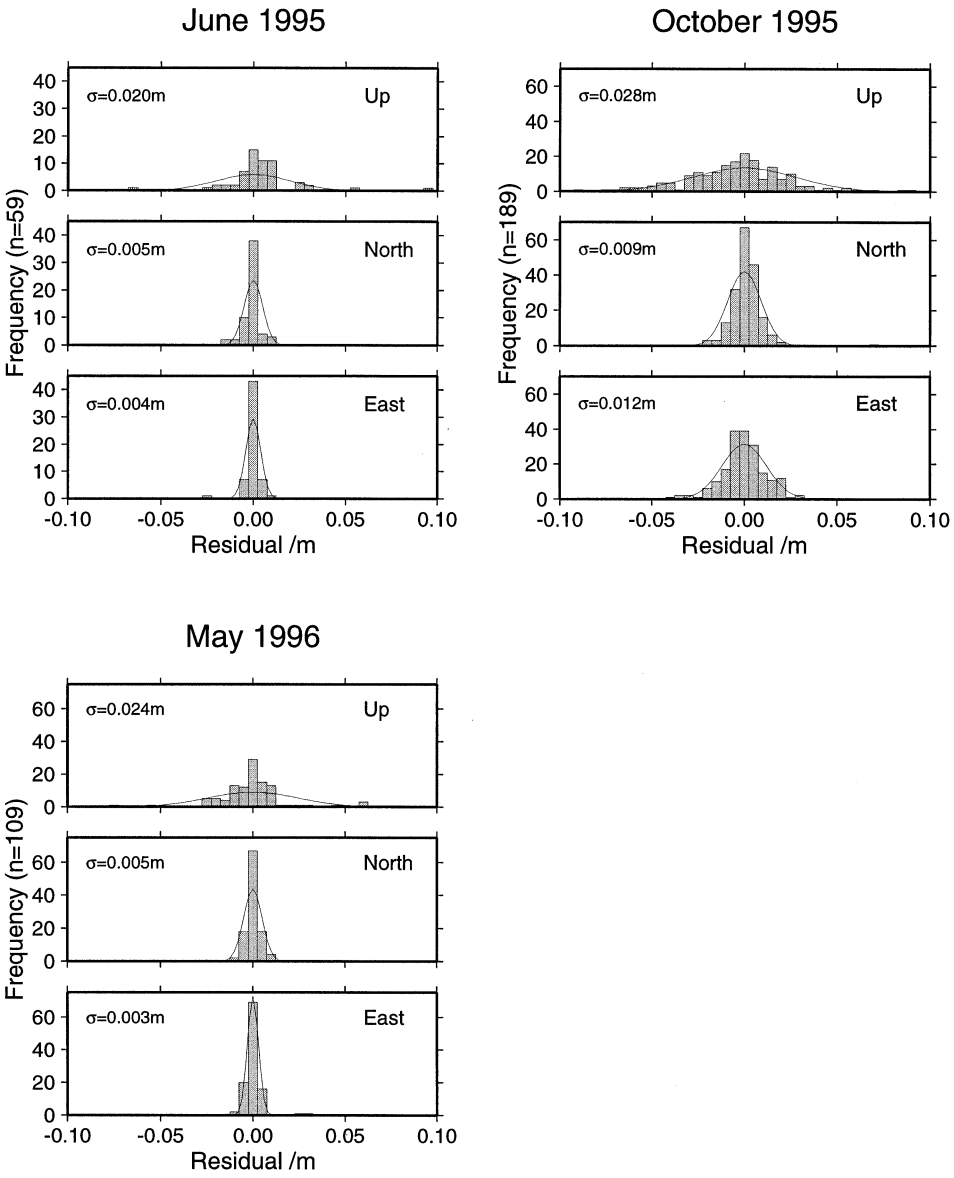

Figure 6. Residuals of daily coordinate sets to campaign solutions 1995–1996 in the local coordinate frame. Vertical scale varies from epoch to epoch.

to all sites surrounding the Gulf of Korinthos using the elastic model of Okada (1985). The model displacements are compatible with our uncorrected observations over the interval 1993–1995, which must include both coseismic and interseismic components; if anything we find that the model slightly overcompensates for the coseismic effects, in that the model displacements (which include coseismic motion only) marginally exceed our observed displacements over the interval May 1993–June 1995 (which include both coseismic and interseismic motion).

Fig. 8 shows changes in baseline length for the period 1991–1996, after coseismic corrections have been applied, between pairs of the most frequently occupied sites, spanning the Gulf. The smooth changes in baseline length demonstrate that our reference frame is maintained from epoch to epoch without scale errors. However, this alone is insufficient to demonstrate that interseismic site velocity vectors are also uniform with time.

Linear site velocities

For epoch campaigns processed using relative GPS, a significant part of the coordinate error at each epoch is due to random (human) error involved in setting up the antenna over the marker. For the vast majority of sites, we have reduced the effect of such errors by performing two or more independent set-ups during each campaign, but in the surveys of 1993 and later, the base station at DION was only set up once and operated continuously throughout the campaign. Thus each campaign coordinate set may be subject to a small global offset caused by set-up errors and short-term local perturbations at DION, and also systematic medium-term tidal, groundwater and atmospheric effects, and errors in local site ties at DION. A simple attempt to fit a uniform velocity through these coordinate sets will therefore be in error.

Instead, we estimate a global network translation at each epoch, except for one reference epoch (in our case 1993

GJI000 14/9/98 12:31:21 3B2 version 5.20
The Charlesworth Group, Huddersfield 01484 517077

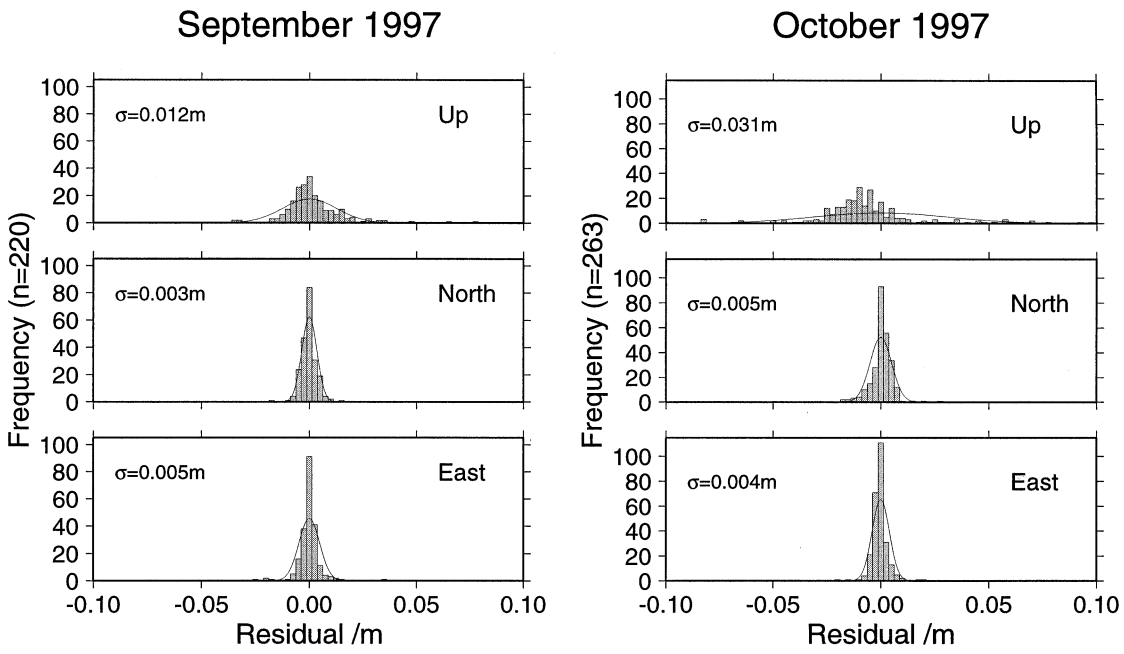

Figure 7. Residuals of daily coordinate sets to 1997 campaign solutions in the local coordinate frame. Vertical scale varies from epoch to epoch. The higher vertical residuals in October 1997 are thought to be the result of using more than one receiver and antenna type at each site during the campaign.

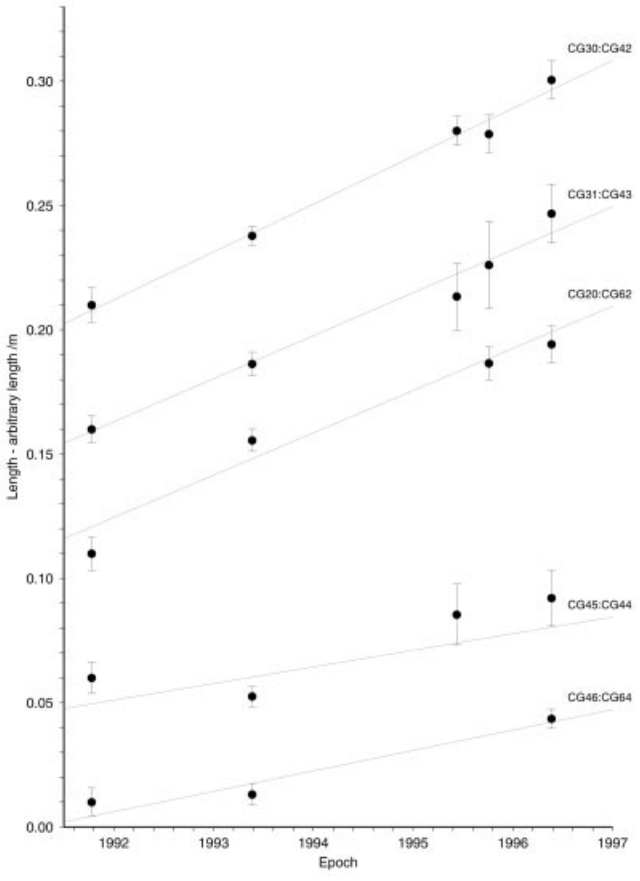

Figure 8. Changes of baseline length 1991–1996 for baselines spanning the Gulf of Korinthos, relative to an arbitrary zero-offset. Site coordinates at epochs later than 1995 June 15 have been corrected for coseismic displacements in the Egion earthquake according to the model of Bernard *et al* (1997). The best-weighted linear fit to each set of baseline length measurements is shown.

because it is the most accurate and complete survey). This procedure introduces two more degrees of freedom per epoch, a small increase on top of the four degrees of freedom per site for velocity determinations. To distinguish global velocity offsets from translation parameters, we fix the velocity of DION. As we wish to determine velocities relative to stable Eurasia, we compute the velocity of DION in our reference frame by subtracting the NNR–Nuvel-1 rigid-body rotation of Eurasia (evaluated at DION) from the ITRF 92 observed velocity for DION. Because the NNR–Nuvel-1 pole of rotation for the Eurasian plate is far away, stable Eurasian predicted velocities vary insignificantly across the CGN, so this method yields velocities of all sites in the network relative to stable Eurasia, subject to uncertainty in the SLR-derived ITRF velocity of DION.

The best-fitting set of translation parameters is determined using iterative least squares by the method of normal equations. Inversion is carried out using a standard singular value decomposition algorithm (Press *et al.* 1992) to ensure numerical stability. The overall measure of goodness of fit is the weighted sum of squares of residuals to the coordinate observations; only sites with three or more epochs of occupation have redundant observations and so contribute to this. In addition to coordinates from the three primary and five partial CGN surveys, we include the coordinates from the 1988 and 1992 GPS resurveys of the 1890s triangulation network (Billiris *et al.* 1991; Davies 1996; Davies *et al.* 1997), which between them include eight CGN sites (11, 16, 18, 21, 44, 48, 54, 59) and were processed using fiducial methods similar to that of the 1989, 1991 and 1993 CGN surveys. We also include coordinates from the two supplemental surveys at DION (site 54) and XRIS (site 16) performed in June and September 1996. In total, 378 pairs of coordinates are used.

Results of this fit for the most frequently observed sites (those around the Gulf of Korinthos) are displayed in Fig. 9. The rms residual at the base station DION is 7.3 mm per

GJI000 14/9/98 12:31:24 3B2 version 5.20
The Charlesworth Group, Huddersfield 01484 517077

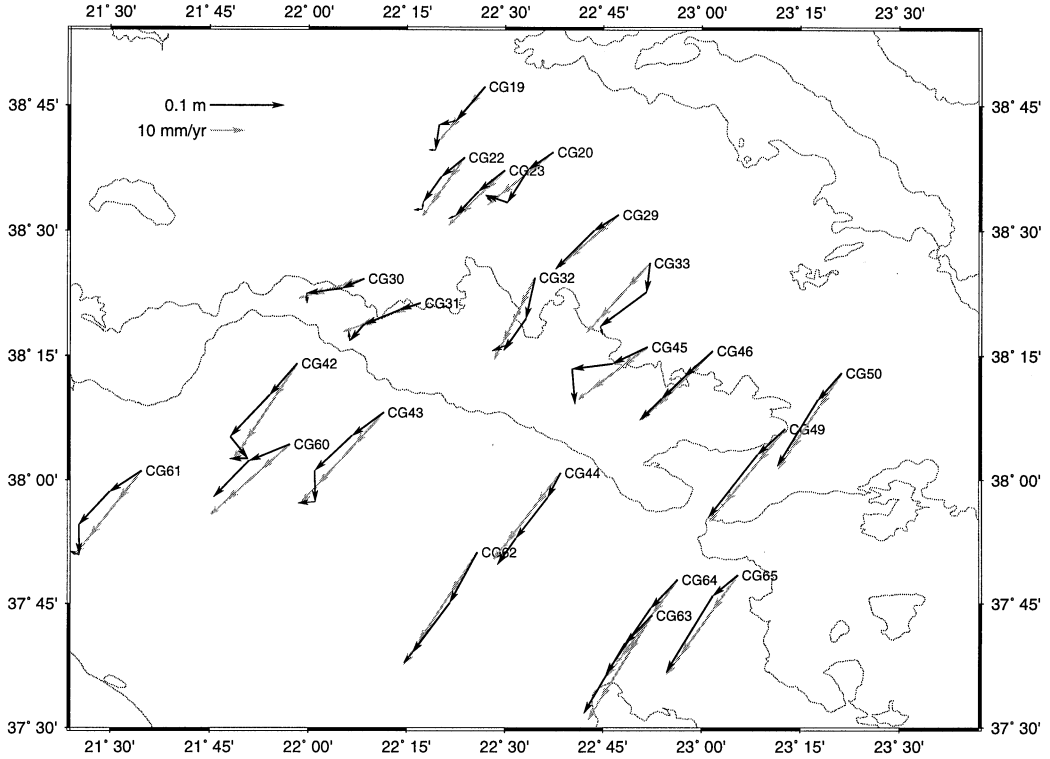

Figure 9. Cumulative displacements relative to stable Eurasia (black arrows) of CGN sites around the Gulf of Korinthos that have been occupied on three to five occasions from 1991–1996 after epoch network translations and coseismic corrections have been applied. The best-fitting linear velocity for each site is shown in grey, with arrow-head positions corresponding to the cumulative displacements from epoch 1991.78 to epochs 1993.39, 1995.44, 1995.76 and 1996.39.

coordinate, which is very similar to the post-1991 rms residual to the uniform velocity fitting, 7.8 mm per coordinate (1.3σ rms weighted residual); that is, the translations required at DION are comparable to the *a posteriori* estimates of coordinate precision at other sites. The former residual provides an estimate of the reference frame noise at each epoch affecting our velocity field, which results from antenna misalignment and/or local perturbations of the DION marker caused by for example groundwater and tidal loading; the latter provides an estimate of typical set-up and other local errors affecting individual site occupations at each epoch. We find that the estimates of coordinate uncertainty from our campaign network adjustments are in general matched by the *a posteriori* rms residuals to our velocity fitting. Coordinate precision improves by half an order of magnitude from 1988/9 (65 mm rms and 35 mm rms respectively) to 1991 (9.4 mm rms), and more gradually thereafter. Because of this, the 1988/9 observations have relatively little effect on the velocities.

If we do not estimate epoch network translations, the post-1991 rms residual to uniform velocity fitting is 19 mm per coordinate (4.1σ rms weighted residual). This decrease of the penalty function (misfit) χ^2 by a factor of three for a small increase in the overall number of degrees of freedom (462 compared with 442 if site velocities are simply fitted to the raw epoch coordinates) demonstrates that the estimation of network offsets results in a highly significant improvement to the fitting of uniform velocities for multi-epoch surveys. This improvement arises because the apparent epoch-to-epoch differences in relative GPS coordinates are in fact highly correlated from site to site. The demonstration of the existence of this systematic error, which can only be detected in experiments with three or more precise survey epochs, should encourage caution in the interpretation of some two-epoch experiments, particularly those in which only one station has an independent velocity constraint.

Fig. 10 and Table 1 show the complete velocity field that we have obtained, relative to stable Eurasia. Three sites (25, 47 and 51) show highly anomalous velocities, which we attribute to marker instability and exclude from further analysis. We observe high rates of extension across the Gulf of Korinthos, particularly in the west, but little extension across the Gulf of Evvia. Sites at the northwestern extent of the network are moving southwest relative to Eurasia, confirming that further deformation must take place to the north and west of Greece, although this latter observation is contingent on the accuracy of the SLR velocity determination of DION with respect to stable Eurasia.

Comparison with other geodetic data

The CGN and the 1890s first-order network have five sites in common or as local eccentric markers of each other (11, 21, 44, 48 and 59; SKOP, KNIM, VALT, MKPG and CLMU), and five other 1890s pillars (MKRH, TMFR, SKYR, PALV and OCHI) are within 5 km or less of CGN sites (10, 13, 40, 45 and 56). In addition, the September 1997 survey provided GPS reoccupations of eight 1890s pillars (HYDR, MILS, MKRH, MYKN, OCHI, SKYR, THRA and VALT), making a total of 14 1890s points with reliable GPS–GPS velocities. In the case of the GPS–GPS data we have explicitly removed local

GJI000 14/9/98 12:31:27 3B2 version 5.20
The Charlesworth Group, Huddersfield 01484 517077

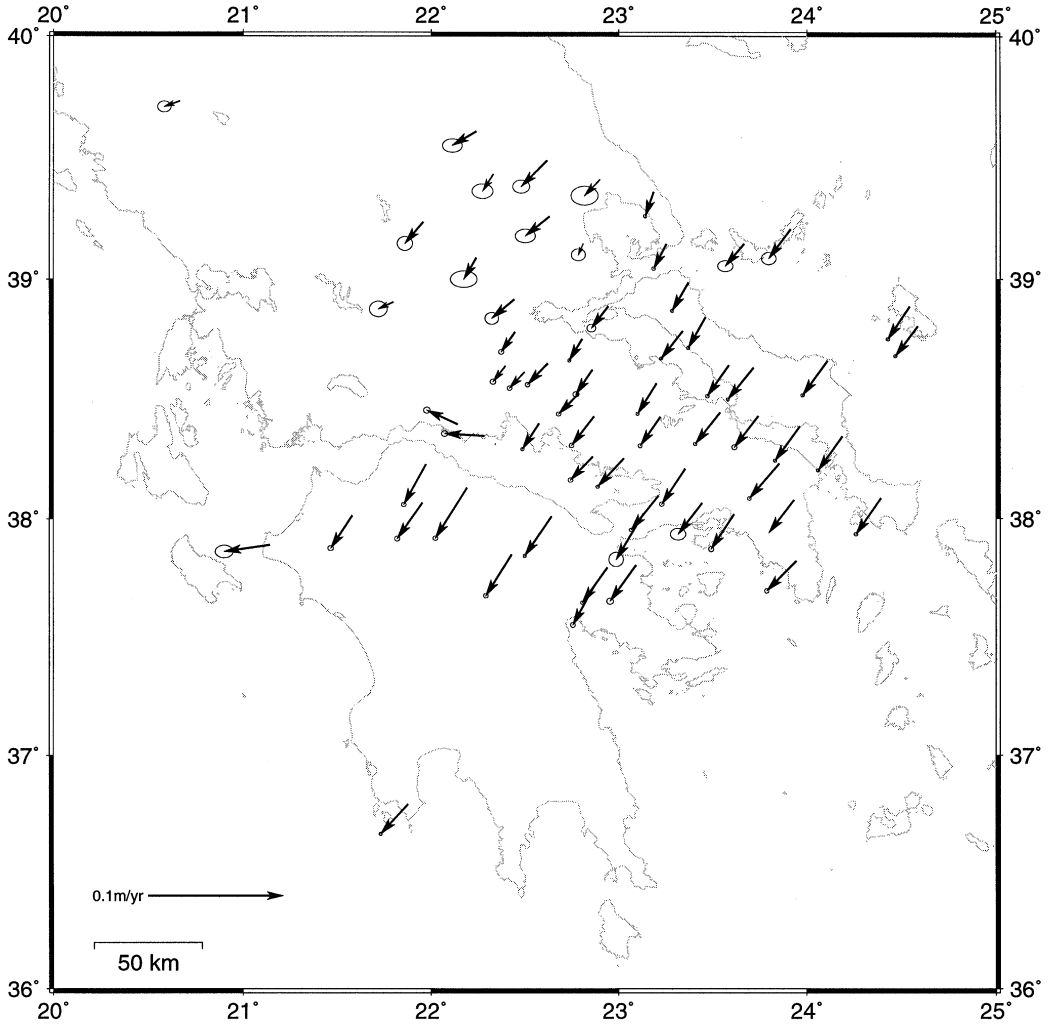

Figure 10. Interseismic velocities of CGN sites, averaged over the interval 1989–1997, after effects of the 1995 Egion earthquake and whole-network translations have been eliminated. All error ellipses represent the 68 per cent confidence interval.

coseismic effects; for the 100 yr data we expect such effects to be close to the level of noise in the original triangulation measurements, and at this scale to have been averaged out over the larger number of earthquakes that have occurred in the interval between surveys. Curtis, England & Davies (1997) find that correcting for local coseismic effects does not significantly improve the fit of the 100 yr displacements to a smooth quadratic field (with the exception of the 1956 Amorgos earthquake, which lies outside our area of interest), supporting this hypothesis.

It is first necessary to address the issue of the reference frame of the 1890s survey. Davies *et al.* (1997) fixed the scale of the network by constraining the change in length of a baseline in the aseismic central Peloponnesos to be zero, and rotating the network such that the velocities at six sites identical or close to CGN sites were equal to their GPS–GPS velocities, in a least-squares sense. Here, we constrain the velocities of the 14 sites to be equal to their GPS–GPS velocities in a least-squares sense, and estimate the scale change and rotation that must be applied to the 1890s network to achieve this. The resulting difference in 100 yr strains compared with the results of Davies *et al.* (1997) is of the order of 0.9 ppm, well within the uncertainty that they attach to their assumptions, so their conclusions are unaffected.

The GPS–GPS and 100 yr velocities at the 14 sites, after the 1890s network has been reoriented, are compared in Fig. 11. Even though the GPS–GPS velocities are in some cases based on as little as two epochs of data 1.6 yr apart, there is a high degree of similarity between the short- and long-term velocities. This is particularly interesting at site 59 (CLMU in the 1890s network), which had been suspected of instability by Billiris *et al.* (1991) on account of its westward motion with respect to the other sites in the Peloponnesos; if the site is unstable, the instability cannot have occurred at an epoch in the interval 1890–1989 but if it exists must instead be a continual process. Instead, we side with Le Pichon *et al.* (1995) in proposing that the reason that site 59 is discrepant with respect to the other sites in the Peloponnesos is that it is coupled to the deformation of the Ionian islands to the west and is not part of the relatively rigid northern Peloponnesos. The rms misfit between the two sets of velocities is 4.9 mm yr^{-1} per component (1.99σ weighted rms residual), indicating that the GPS–GPS and 100 yr velocity fields cannot reliably be distinguished. This can also be seen qualitatively in Fig. 12, in

GJI000 14/9/98 12:31:30 3B2 version 5.20
The Charlesworth Group, Huddersfield 01484 517077

Table 1. Interseismic velocities of CGN sites relative to a non-rotating stable European reference frame, averaged over the interval 1989–1997, after effects of the 1995 Egion earthquake and whole-network translations have been eliminated. Velocities and their errors (1σ) are given in mm yr^{-1}.

Site	Lon °E	Lat °N	V_E	σ_E	V_N	σ_N	Site	Lon °E	Lat °N	V_E	σ_E	V_N	σ_N
01	22.62	39.49	−19.4	4.2	−19.3	3.2	34	23.22	38.43	−14.9	1.0	−21.3	1.0
02	22.24	39.61	−17.9	4.9	−10.4	3.3	35	23.54	38.45	−18.4	0.9	−23.3	0.8
03	22.33	39.43	−8.0	5.2	−12.5	3.6	36	23.59	38.64	−16.0	0.9	−22.8	0.9
04	22.90	39.41	−11.6	6.7	−11.9	4.6	37	23.72	38.63	−19.0	0.8	−23.4	0.8
05	23.19	39.36	−6.2	0.9	−17.9	0.8	38	24.11	38.66	−18.4	0.9	−25.5	0.8
06	21.96	39.24	−13.6	3.8	−15.9	3.4	39	24.54	38.89	−16.1	0.9	−24.3	0.8
07	22.63	39.26	−18.0	5.0	−14.4	3.3	40	24.59	38.80	−16.4	0.8	−22.0	0.8
08	22.24	39.09	−9.3	6.6	−15.9	4.1	41	23.74	38.43	−17.7	1.3	−23.1	1.2
09	22.81	39.15	−3.6	3.5	−8.2	2.9	42	21.97	38.23	−16.5	1.2	−29.7	1.0
10	23.25	39.15	−9.4	0.9	−18.2	0.9	43	22.19	38.13	−23.6	1.2	−37.4	1.1
11	23.67	39.15	−13.9	3.8	−16.4	2.7	44	22.64	38.01	−20.0	0.8	−29.2	0.8
12	23.91	39.21	−16.2	3.6	−21.6	3.0	45	22.86	38.26	−16.7	1.2	−17.4	1.1
13	21.80	38.91	−11.1	4.4	−5.1	3.8	46	23.03	38.25	−19.6	0.9	−21.0	0.8
14	22.44	38.92	−16.8	3.4	−14.0	2.9	48	23.13	38.02	−20.2	3.6	−33.8	3.5
15	22.94	38.89	−12.5	2.2	−16.2	1.9	49	23.21	38.10	−20.4	0.9	−25.4	0.8
16	21.88	36.79	−20.4	0.8	−22.0	0.8	50	23.35	38.21	−17.4	1.1	−26.2	1.1
17	23.37	38.99	−12.1	0.8	−20.9	0.8	52	23.96	38.39	−18.4	0.8	−25.5	0.8
18	20.66	39.73	−11.4	3.3	−4.2	2.7	53	23.85	38.23	−22.1	0.9	−25.7	0.9
19	22.45	38.78	−10.2	1.3	−14.5	1.2	54	23.93	38.08	−18.5	0.0	−24.2	0.0
20	22.62	38.65	−15.0	1.1	−15.7	1.1	55	24.19	38.35	−17.9	0.8	−25.3	0.8
21	22.81	38.75	−9.6	0.8	−15.8	0.8	56	24.39	38.09	−18.4	0.9	−26.7	0.9
22	22.40	38.64	−9.2	1.4	−11.7	1.3	57	23.44	38.07	−17.8	3.8	−23.1	2.9
23	22.50	38.61	−11.2	1.2	−11.8	1.1	58	23.61	38.02	−17.0	1.3	−25.7	1.3
24	22.86	38.62	−12.3	1.5	−18.1	1.3	59	21.14	37.89	−33.7	4.4	−4.9	3.1
26	23.34	38.78	−16.0	0.8	−20.3	0.7	60	21.95	38.07	−18.7	1.3	−26.5	1.2
27	23.46	38.84	−12.8	0.8	−22.7	0.8	61	21.58	38.01	−16.0	1.4	−24.2	1.2
28	23.20	38.57	−14.0	0.8	−22.4	0.8	62	22.43	37.85	−19.3	1.2	−30.6	1.1
29	22.79	38.53	−15.2	1.1	−15.3	1.0	63	22.88	37.72	−16.6	1.2	−30.1	1.2
30	22.14	38.40	−22.9	1.6	10.5	1.5	64	22.94	37.79	−18.7	0.8	−26.0	0.8
31	22.28	38.35	−29.6	1.6	1.7	1.4	65	23.09	37.80	−19.3	1.7	−26.6	1.5
32	22.58	38.40	−12.4	0.9	−18.9	0.8	66	23.94	37.82	−21.8	1.1	−22.1	1.1
33	22.87	38.43	−16.6	1.2	−21.3	1.1							

which both velocity fields are shown in their entirety. We therefore conclude that at the scale of several tens of kilometres our short-term GPS site velocity estimates (corrected for coseismic effects) are representative of the longer-term site velocity over 100 years. Accordingly, we combine the entire set of GPS and triangulation coordinate data into a single set of site velocity estimates.

The 100 yr interval, although shorter than the seismic cycle for an individual fault segment, encompasses many earthquakes within the region as a whole, so we expect the 100 yr velocities (and therefore the GPS–GPS velocities) to be representative of the much longer term. Our result suggests that the correspondence between present-day and very long-term crustal deformation on the global scale, that is plate tectonic motions (Argus & Gordon 1990; DeMets *et al.* 1994), may also apply at the scale of a few tens of kilometres, even in deforming continental regions where the concept of rigid plates does not apply.

Sites 16, 18 and 54 of the CGN coincide with SLR sites XRIS, KRTS and DION respectively. SLR observations have been made at these monuments four times during the interval 1986–1992 (Smith *et al.* 1994; Le Pichon *et al.* 1995). Independent dual-frequency GPS observations have also been made four times during the period 1989–1993 at these sites and at monuments coincident with sites 13, 42, 59 and 61 of the CGN (Kahle *et al.* 1995, 1996). The velocities derived from these sets of observations can be compared with those obtained in this study from between three and 11 occupations with GPS between 1989 and 1997 (Fig. 13). At the SLR sites DION and XRIS, there is good agreement between this study and the previous GPS and SLR work. However, at KRTS (site 18), we find evidence of significant west-southwestward motion that is absent from the studies of Le Pichon *et al.* (1995) and Kahle *et al.* (1995) (the result of Smith *et al.* (1994) is not shown because it is affected by the known blunder at KRTS reported in *CDDIS Bulletin,* **9**(6), 7). The implication of our result is that there is in fact a region of on-going deformation between KRTS and the stable European plate, a view that is borne out by the seismicity in this area (Fig. 1). At sites 13, 42 and 61, our results tally with the GPS results of Kahle *et al.* (1995), although at site 42 [for which we have five epochs of observation compared to two reported in Kahle *et al.* (1995)] we find an increased southwesterly interseismic velocity that implies little or no deformation in the northern Peloponnesos between sites 42 and 61. At site 59 we find considerably more westward motion than Kahle *et al.* (1995), implying that the site is more strongly linked to the Ionian islands than to the northern Peloponnesos.

Unified strain field

From the unified velocity field, we proceed to evaluate the strain field in Greece. Rather than fit spline or polynomial functions to the entire velocity field, which can result in either

GJI000 14/9/98 12:31:53 3B2 version 5.20
The Charlesworth Group, Huddersfield 01484 517077

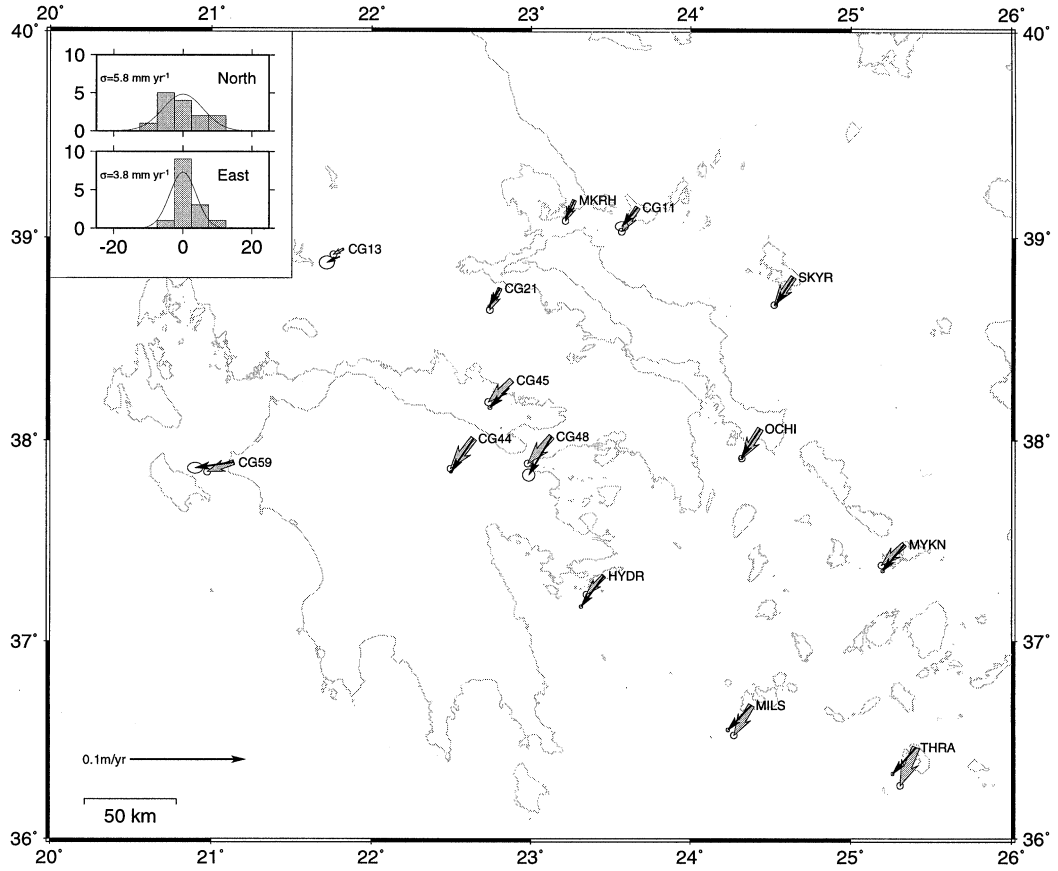

Figure 11. Comparison of velocities of CGN sites common to the 1890s network, or within 5 km of 1890s sites, over the periods 1892–1988/92 (shaded arrows, after 1890s triangulation has been rescaled and reoriented as decribed in the text) and 1989–1997 (black arrows). Error ellipses represent 68 per cent confidence limits. Inset shows the histograms ($n=14$) of east and north velocity differences between the two sets of site velocities.

excessive damping or instability of the interpolation, we have made discrete estimates of the velocity gradient tensor at points on a regular grid, using the velocities of a minimum of four sites within 40 km of each grid point. If only three such sites exist we do not compute a velocity gradient tensor because such an estimate, being even-determined, is liable to instability, particularly if two of the three sites are much closer to each other than to the third. We have estimated velocity gradient tensors for a range of radii of interest and find that a 40 km radius enables good coverage of the survey area without causing excessive smoothing. Our grid is aligned along 020°, perpendicular to the strike of the main visible tectonic features of the region (the Gulfs of Korinthos and Evvia).

Although the method of calculating strains described above is in essence local, several consistent trends can be seen (Fig. 14). Strain rates thoughout the Gulf of Evvia and northern part of the network are relatively low, but significant, and show generally north–south extension (typically around 0.06 ± 0.03 ppm yr^{-1}); extensional strain rates within the southern part of the network (Peloponnesos) are similarly low. However, strain rates in the central part of the network across the Gulf of Korinthos are significantly higher, reaching 1.12 ± 0.05 ppm yr^{-1} in the western Gulf. High strain rates are also seen at the northern and northwestern extremities of the study area. It is interesting to note that these high strains correspond to the region of the 1954–1955 Volos earthquakes.

The contrast in extensional strain rates between the Gulfs of Korinthos (0.15 ± 0.02 to 1.12 ± 0.05 ppm yr^{-1}) and Evvia (typically 0.06 ± 0.03 ppm yr^{-1}) is striking. Both gulfs are significant geomorphological features that have been tectonically active throughout the Quaternary and have experienced large earthquakes in the last century (Ambraseys & Jackson 1990), although seismic activity in the Gulf of Evvia has been lower in the last 30 years. It is possible that earthquake recurrence times on individual fault segments in the Gulf of Korinthos are shorter, to accommodate higher strain rates in the underlying lithosphere. Alternatively, there may be fewer active fault segments taking up the strain across the Gulf of Evvia. The similarity in the relief in the two regions may support the latter suggestion, but the historical record of seismicity is not sufficiently long or precise to distinguish between these hypotheses.

A high degree of consistency is also exhibited by the geodetic rigid-body rotation rate estimates (Fig. 15), where the rotation rate $\dot{\omega}$ is defined by

$$\dot{\omega} = \frac{1}{2}(\boldsymbol{L} - \boldsymbol{L}^{\mathrm{T}}) \tag{1}$$

for a velocity gradient tensor $\boldsymbol{L}$. Variation in the geodetic rotation rate within areas previously postulated to be rigid blocks indicates that such regions are in fact deforming

GJI000 14/9/98 12:32:17 3B2 version 5.20
The Charlesworth Group, Huddersfield 01484 517077

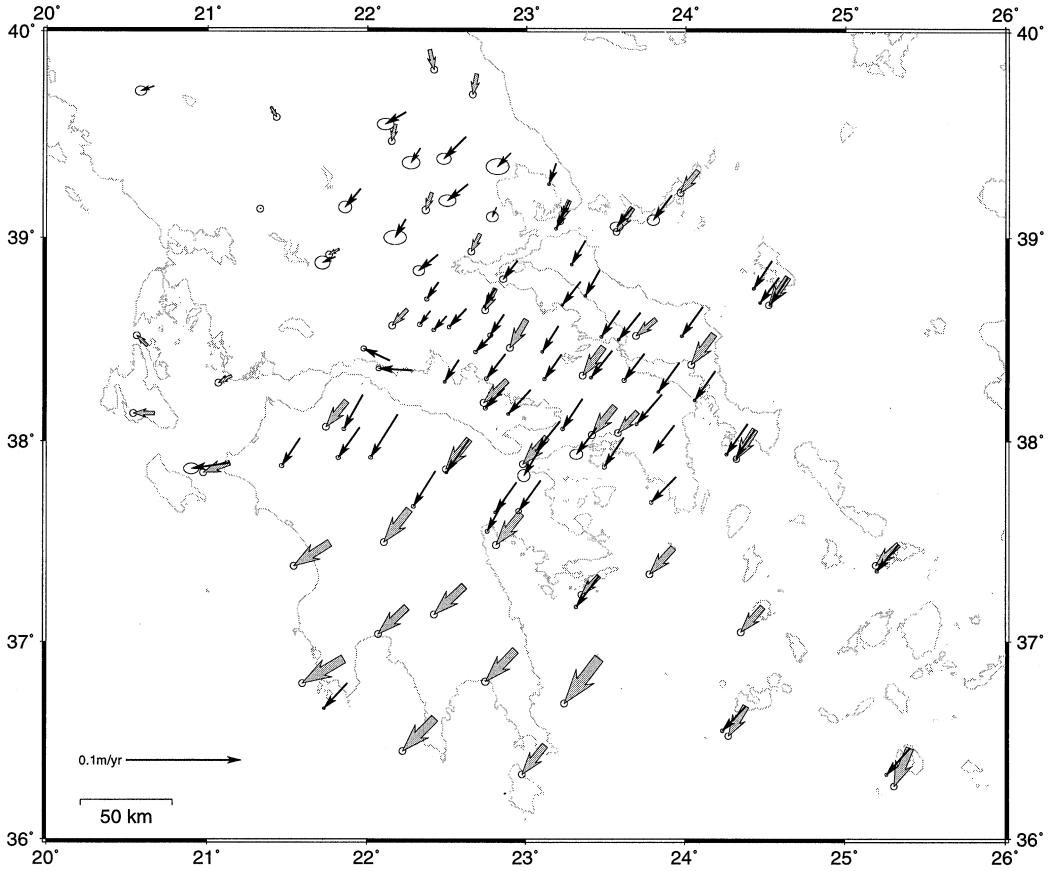

Figure 12. Velocities of monuments in central Greece, determined over an approximate 100 yr interval by triangulation and GPS (shaded arrows, after 1890s triangulation has been rescaled and reoriented as decribed in the text) and over intervals of no more than 8 yr by GPS alone (black arrows). Error ellipses represent 68 per cent confidence limits.

and therefore care must be taken not to overinterpret rigid-block models that describe only first-order features of the deformation field.

VARIATION OF STRAIN WITHIN THE GULF OF KORINTHOS

We now turn to the deformation in the Gulf of Korinthos as this is the best-surveyed part of central Greece. Interseismic strain within the Gulf of Korinthos is overwhelmingly pure north–south extensional strain, and increases from 0.15 ± 0.02 ppm yr^{-1} in the east to 1.12 ± 0.05 ppm yr^{-1} in the west. These values from our gridding method are commensurate with those obtained for discrete triangular regions spanning the Gulf by Davies *et al.* (1997) using only the 100 yr data set.

In this section we wish to study the correspondence between short-term and 100 yr deformation and the variation of strain within the Gulf in greater detail. We investigate the change in extension rate across the Gulf of Korinthos by considering the relative velocities of sites on either side of the Gulf. It can be seen from Figs 9 and 10 that the sites on the northern Peloponnesos bordering the Gulf of Korinthos are moving with very similar velocities. We again estimate smoothed velocities for CGN sites, but this time constrain the sites on the southern side of the Gulf of Korinthos to be stationary. Use of this constraint is validated by the observation that the rms residual to the fit is increased only marginally from the previous estimation, confirming again that the northern Peloponnesos is deforming very slowly and that extension is primarily localized within the Gulf of Korinthos.

Site velocities and cumulative displacements subject to the Peloponnesos-fixed constraint are shown in Fig. 16. The velocities of sites north of the Gulf are nearly perpendicular to the strike (110°) of the Gulf, but exhibit a small amount of left-lateral shear. We take the component of site velocity normal to the Gulf, along 020°, and display this extension rate as a function of distance along the Gulf (Fig. 17). The extension rate increases smoothly from east to west, independently of whether sites are located close to or away from the Gulf. This provides further confirmation that deformation is localized to first order within the Gulf.

Also given in Fig. 17 are the velocity components of 1890s sites calculated similarly. The data are in very good agreement, although the variation in extension rate of the 1890s data is marginally smaller than that of the CGN data. This reconfirms, on a local scale, that short-term GPS studies are capable of determining estimates of crustal motions that are valid over far longer timescales.

DISCUSSION

Because the Gulf of Korinthos is surrounded by one of the more populous parts of Greece, it has a well-known history

GJI000 14/9/98 12:32:41 3B2 version 5.20
The Charlesworth Group, Huddersfield 01484 517077

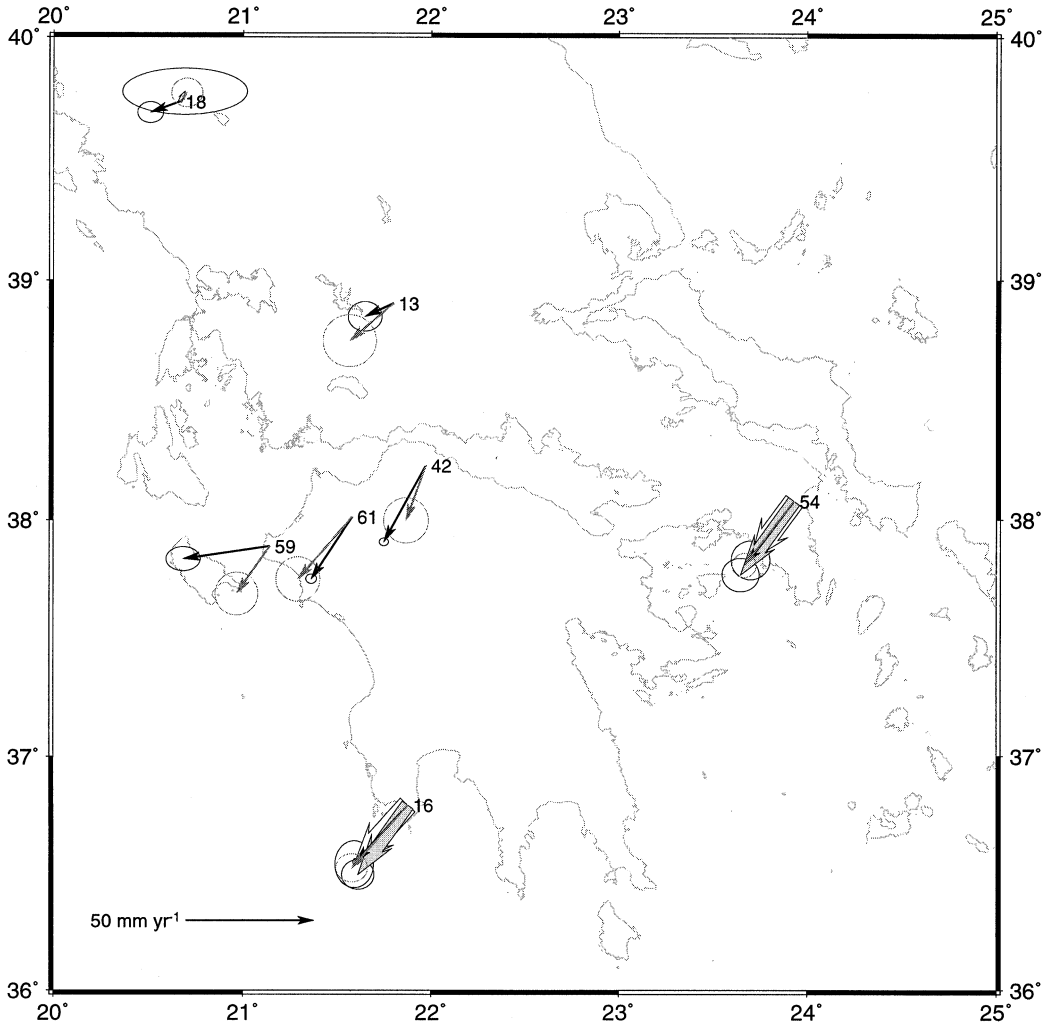

Figure 13. Velocities of monuments in central Greece, with respect to northern Europe, as determined from four SLR occupations 1986–1992 (Le Pichon *et al.* 1995, large open arrows and Smith *et al.* 1994, large shaded arrows, not at site 18), from two dual-frequency GPS occupations 1989–1993 (Kahle *et al.* 1995, small grey arrows) and from three or more dual-frequency GPS occupations within the period 1989–1997 (this study, black arrows). Error ellipses represent 68 per cent confidence limits. Note that we obtain a significant southwestward velocity for site 18 (KRTS), in contrast with Kahle *et al.* (1995) and Le Pichon *et al.* (1995), who obtain null vectors.

of earthquakes (Ambraseys & Jackson 1990, 1997; Papazachos 1990; Papazachos & Papazachos 1989), and it is of interest to compare the geodetic extension rate with the long-term rates of seismicity and fault movement. We have covered this from the point of view of seismic hazard elsewhere (Clarke *et al.* 1997); here we concentrate on the tectonic implications of our results.

Armijo *et al.* (1996) have modelled terrace uplift in the region of the Xylokastro Fault (22.75°E) and obtained Quaternary extension rates of 5–9 mm yr^{-1} for this part of the Gulf. This value is commensurate with our geodetic estimates, which, although shorter-term, do not rely on any mechanical model of fault behaviour. Armijo *et al.* (1996) also predicted from their mechanical model, on the basis of less reliable uplift observations reported elsewhere, that the Helike Fault (22.25°E) has slipped throughout the Quaternary at a lower rate of 3–8 mm yr^{-1}. This contrasts with our geodetic finding of significantly higher extension rates in the western Gulf of Korinthos over both 5 yr and 100 yr timescales, although if offshore faults take up a significant proporion of the deformation (as in the recent Galaxidi and Egion earthquakes) then this discrepancy may be resolved.

Le Pichon *et al.* (1995) argue, on the basis of the greater width of the eastern Gulf of Korinthos, that the amount of finite extension is greater there than in the western Gulf of Korinthos. A plausible objection to this argument is that the crustal thickness prior to extension may not have been the same at both ends of the Gulf, so lower topography will not necessarily coincide with greater crustal stretching. Throughout the rest of central and northwestern Greece, higher topography in the west gives way to lower topography in the east, implying that the pre-rift surface elevation was not uniform. However, the difference in pre-rift topography is probably insufficient to offset the present-day difference in width of the Gulf, so it is likely that finite extension does indeed decrease to the west. The instantaneous extension rates in the western Gulf of Korinthos, which we find to be larger than those in the east, can therefore not have been maintained over the last 2.5–3 Myr (Doutsos & Poulimenos 1992; Armijo *et al.* 1996) since the start of rifting, or even the most recent 1 Myr rifting

GJI000 14/9/98 12:32:55 3B2 version 5.20
The Charlesworth Group, Huddersfield 01484 517077

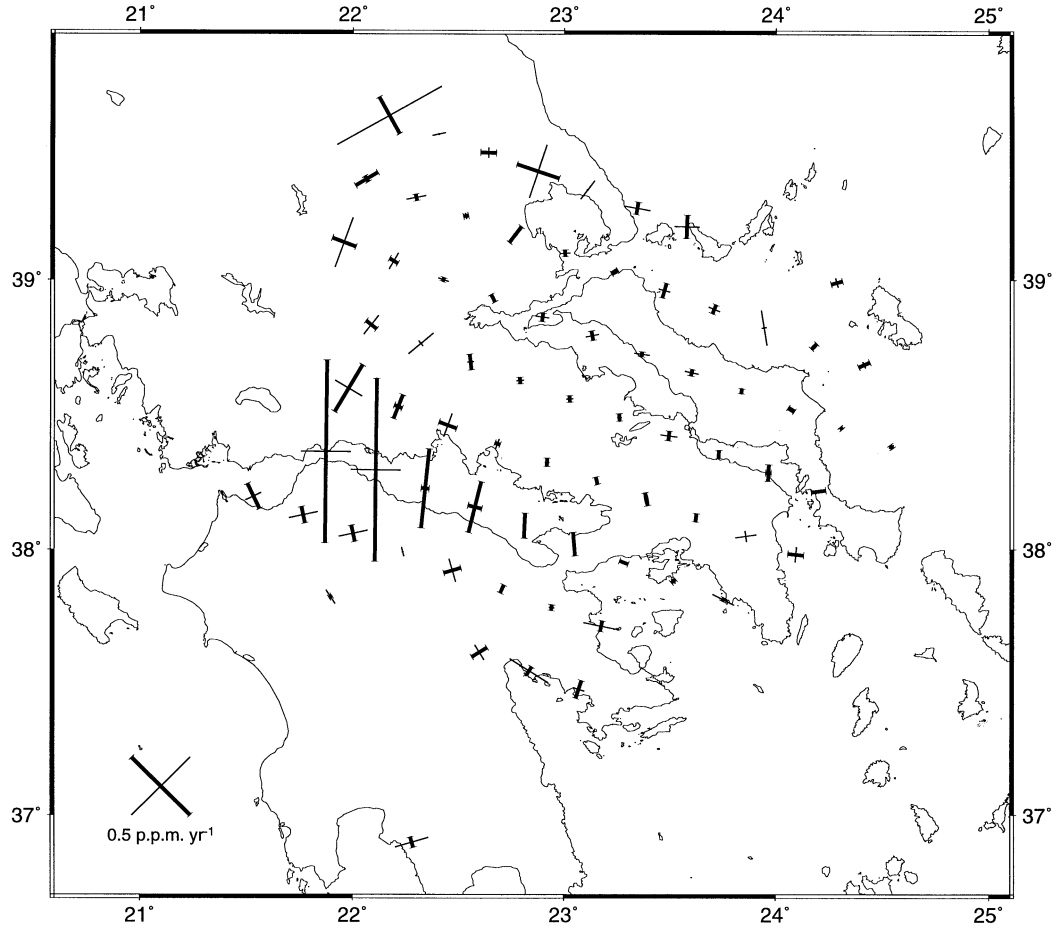

Figure 14. Principal strain axes computed at points on a regular grid aligned along 020° using velocity estimates at sites within 40 km (see text). Thick lines denote extensional strain, thin lines compressional strain. Errors are typically less than 0.05 ppm yr^{-1}.

episode (Armijo *et al.* 1996). It seems likely that extension has propagated westwards during the evolution of the Gulf.

Ambraseys & Jackson (1997) have published a catalogue of earthquakes in the Gulf of Korinthos since 1694, complete for events of magnitude $M_s \geq 6$. Using the strain–moment tensor relationship of Kostrov (1974), they deduced long-term seismic extension rates of 5.3 mm yr^{-1} for the western Gulf and 5.8 mm yr^{-1} for the eastern Gulf, although they suggest that the contribution of $M_s<6$ earthquakes may double these values. In the east, the seismic extension rate is compatible with short-term and 100 yr geodetic observations (Fig. 17), but in the west, the geodetic extension rate is considerably higher, even if smaller earthquakes are taken into consideration. There are two possible ways to increase the extension rate estimated from seismicity in the western Gulf of Korinthos.

(1) A decrease in the seismogenic layer thickness from east to west. The relationship of Kostrov (1974) states that for a volume of material V with modulus of elasticity μ, the components $\dot{\epsilon}_{ij}$ of the strain rate tensor are given by

$$\dot{\epsilon}_{ij} = \frac{1}{2\mu Vt} \sum_{n=1}^{N} M_{ij}^{n}, \tag{2}$$

where M_{ij}^{n} are the elements of the moment tensors of earthquakes within the volume occurring during a representative period t. One way to increase $\dot{\epsilon}_{ij}$ is by increasing the scalar moments of the earthquakes; the other is by decreasing the volume, or for a given area the thickness, of the seismogenic layer. The latter seems unlikely; microseismicity (Rigo *et al.* 1996) and aftershock (King *et al.* 1985) studies in the western and eastern Gulf, respectively, yield similar source depths. Body-wave modelling of recent large earthquakes (e.g. Taymaz *et al.* 1991) cannot distinguish systematic differences in rupture initiation depth between west and east.

(2) An increase in the contribution of $M_s<6$ earthquakes in the western Gulf of Korinthos. Again, this seems unlikely: if smaller earthquakes contribute such that geodetic and seismic extension rates agree in the western Gulf, then the seismic extension rate in the eastern Gulf of Korinthos would be far higher than the geodetic, whereas the two are actually in agreement. Smaller earthquakes in the ISC catalogue for 1964–1994 are roughly evenly distributed throughout the Gulf (Fig. 1), and the frequency distributions of shallow earthquakes in the eastern and western parts of the Gulf are virtually identical (Fig. 18). The empirical relationship between the number of earthquakes $N(M)$ having a magnitude M_s greater than M (Gutenberg & Richter 1954),

$$\log N(M) = a - bM, \tag{3}$$

should properly be replaced by a relationship using scalar moments, M_0:

$$\log N(M_0) = A - B \log M_0, \tag{4}$$

GJI000 14/9/98 12:33:08 3B2 version 5.20
The Charlesworth Group, Huddersfield 01484 517077

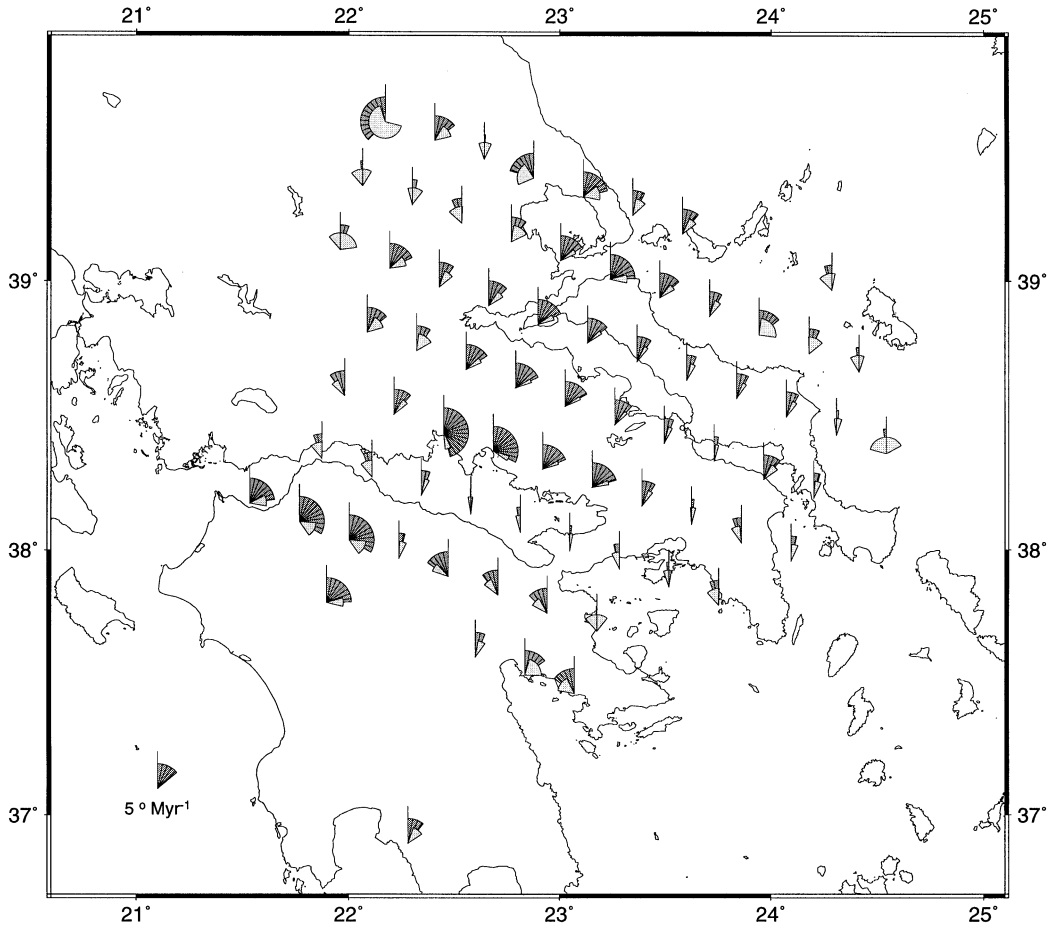

Figure 15. Geodetic rigid-body rotations computed at points on a regular grid aligned along 020° using velocity estimates at sites within 40 km (larger heavily shaded symbols; see text). Error wedges (smaller, more lightly shaded symbols) represent 68 per cent confidence limits.

because M_0 has a uniform interpretation for both small and large earthquakes. This relationship can be used to assess the contribution of smaller earthquakes to the total strain release. The 30 yr ISC earthquake catalogue suggests that recent earthquakes of $M_s \geq 6$ at both ends of the Gulf of Korinthos have been more frequent than expected either from the adoption of a B-value of 2/3, or from the 100 yr and 300 yr catalogues (Ambraseys & Jackson 1990, 1997), which lie, within error, on the expected frequency–magnitude distribution (Fig. 18). Clarke *et al.* (1997) used the 100 yr catalogue for their quantitative analysis; using the $B = 2/3$ standard distribution they found that the small earthquakes in the western Gulf of Korinthos were insufficient to account for the discrepancy.

Failing either of the above, a third possibility is that significant aseismic strain occurs in the western Gulf of Korinthos. More detailed monitoring of the geodetic strain and seismicity in the western Gulf of Korinthos is necessary to test this hypothesis.

CONCLUSIONS

We have established a dense network in central Greece to study crustal deformation using GPS, and demonstrated that measurements of strain made over a few years are compatible with 100 yr measurements, and provide as good a constraint on long-term strain as the latter. Our network has been disturbed by coseismic strain due to the 1995 June 15 Egion earthquake, but with the aid of independent geodetic, seismological and tectonic data (Bernard *et al.* 1997) we have successfully removed these effects by elastic modelling. We have computed smoothed velocities for our sites by eliminating the spatially correlated component of positional error at each epoch. This reference frame noise is a highly significant contribution to the total error budget, and can only be estimated when observations have been made at three or more epochs, as in this study.

We have estimated strains at points on a regular grid using the velocities of neighbouring stations, and show that although low strains are present throughout the network, regions of high strain are localized at a scale significantly smaller than that of the network. In both the short-term and 100 yr geodetic data sets, high strains are observed within the Gulf of Korinthos that increase towards its western end. Long-term seismic extension rates in the eastern and western Gulf of Korinthos are similar, and so it is possible that significant aseismic crustal strain occurs in the western Gulf of Korinthos. In addition, the marked contrast in geodetic strain rates between the geomorphologically and seismically similar gulfs of Korinthos and Evvia implies that some degree of localization of lithospheric strain may be present under the former.

GJI000 14/9/98 12:33:52 3B2 version 5.20
The Charlesworth Group, Huddersfield 01484 517077

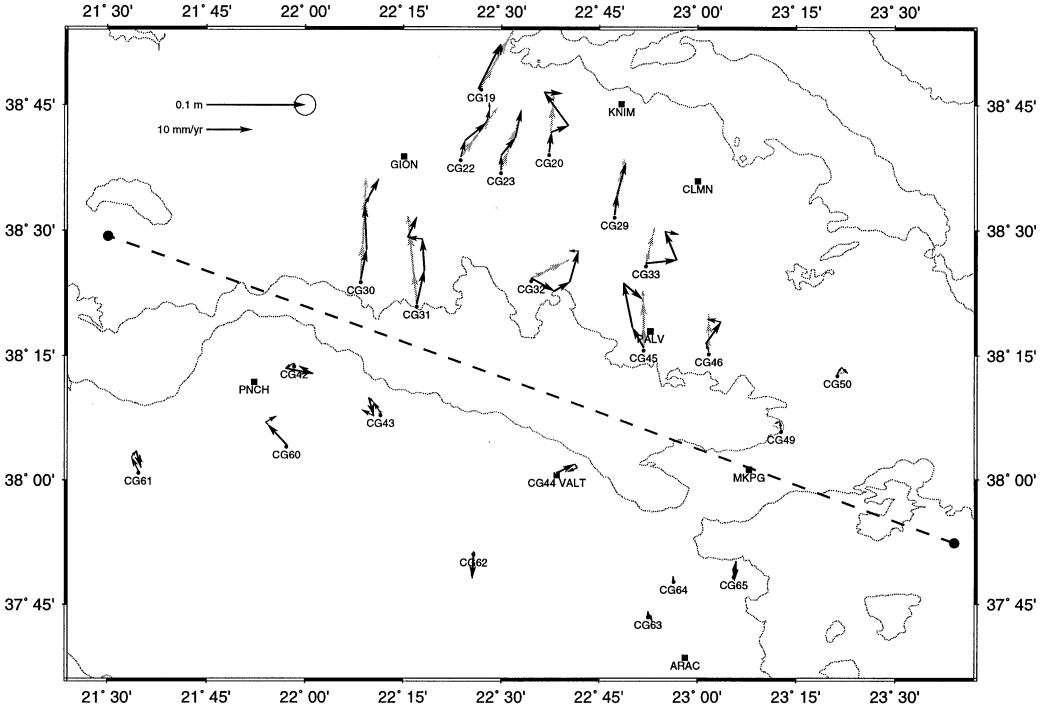

Figure 16. Cumulative displacements over the interval 1991–1996 for CGN sites, relative to the Peloponnesos, after correction for coseismic strain due to the 1995 June 15 Egion earthquake and epoch network translations such that sites on the northern Peloponnesos are on average stationary. Actual epoch-to-epoch displacements after translation (black arrows) show insignificant motions of Peloponnesos sites, but sites north of the Gulf show steady motion perpendicular to the Gulf. Sites in the 1890s network are shown as squares, and the dashed line (azimuth 110°) is the line of section in Fig. 17.

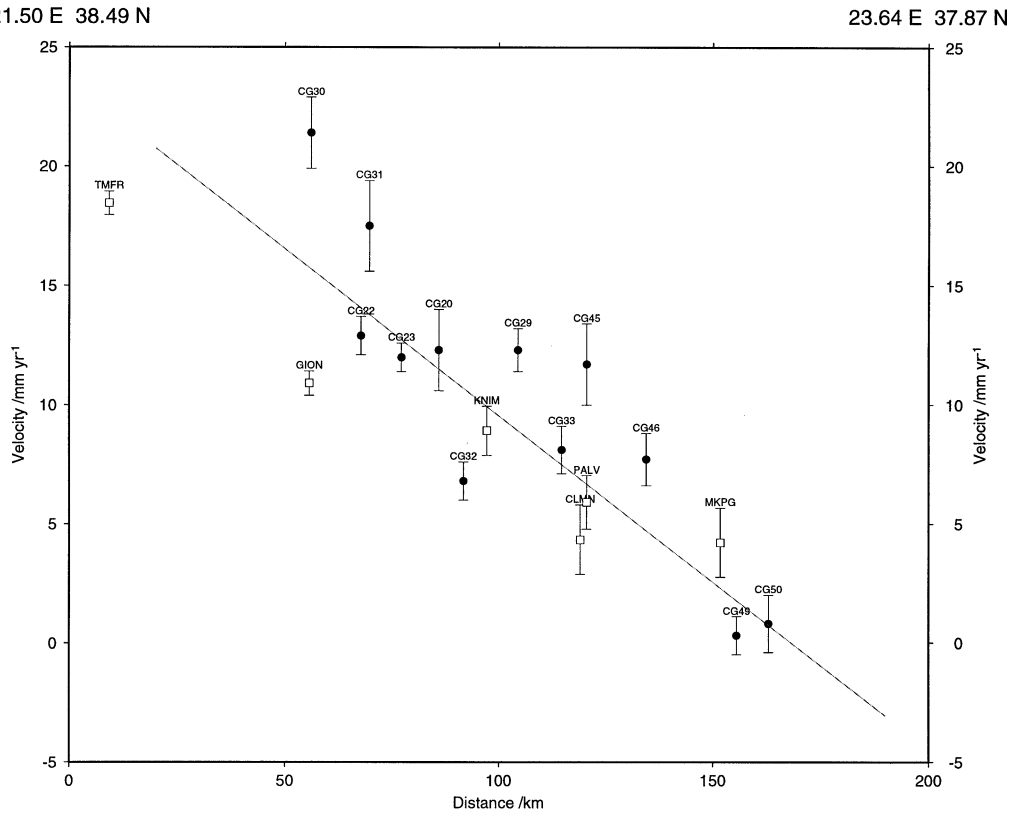

Figure 17. Velocity components 1991–1996 (filled circles) along 020° for CGN sites north of the Gulf of Korinthos, relative to the Peloponnesos. The *x*-axis shows eastward distance along the line of section (azimuth 110°) in Fig. 16. Also shown are the velocity components along 020° for 1890s sites relative to the Peloponnesos (open squares). The best-fitting weighted linear trend to the CGN data is shown.

GJI000 14/9/98 12:33:56 3B2 version 5.20
The Charlesworth Group, Huddersfield 01484 517077

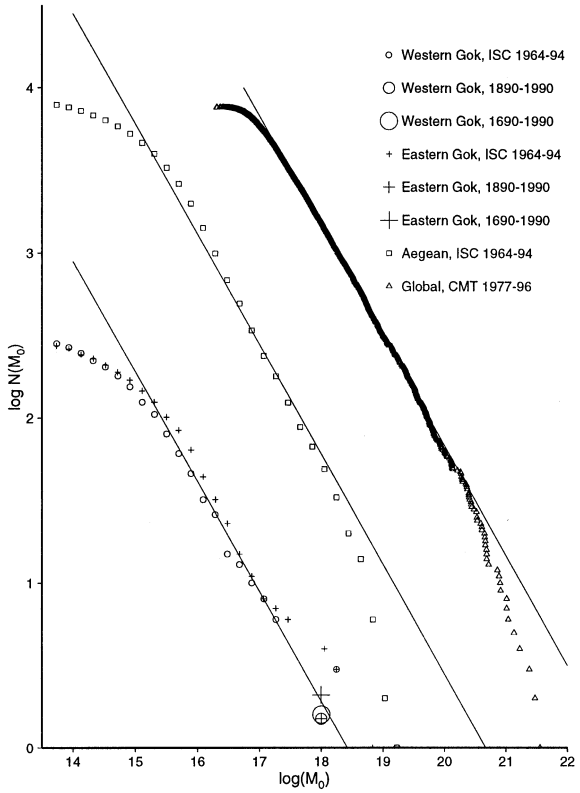

Figure 18. Numbers of shallow earthquakes $N(M_0)$ having a scalar moment greater than M_0 for events of $M_b \geq 3.5$ in the eastern and western Gulf of Korinthos, and throughout the Aegean extensional region, from the ISC catalogue 1964–1994. Also shown is the corresponding plot for shallow earthquakes of $M_b \geq 4.5$ in the global Harvard CMT catalogue 1977–1996. The 100 yr ($M_s \geq 5.8$) and 300 yr ($M_s \geq 6$) catalogues have been normalized to 30 yr seismicity rates for each half of the Gulf. Best-fitting lines with $B=2/3$ are shown. We use the M_b–M_s relationship determined for Mediterranean earthquakes by Giardini, di Donato & Boschi (1997).

ACKNOWLEDGMENTS

Fieldwork was supported by the EC Science Stimulation Programme (Grant SC1000020), the Natural Environment Research Council (Grants GR3/10399A and GR3/10383), ETH Zürich (Grant 07749/41.0820.05) and the Earthquake Planning and Protection Organisation of Greece. We thank the staff and students of the authors' institutions, particularly NTUA, the NERC Geophysical Equipment Pool and A. Wright (Global Surveys Ltd) for their assistance with fieldwork. We also thank D. Hatzfeld and colleagues for their participation in the October 1995 campaign, and M. A. Moore for her contribution to processing the data. We are grateful to N. N. Ambraseys, J. A. Jackson and P. Bernard for making seismological data available to us in advance of publication. PJC and RRD acknowledge NERC studentships during the tenure of which much of this work was carried out.

REFERENCES

Agatza-Balodimou, A.M., Briole, P., Lyon-Caen, H., Mitsikaki, C., Rigo, A., Ruegg, J.-C., Papazissi, K. & Veis, G., 1995. Recent developments in deformation studies from geodetic data in the Corinthian Gulf (Greece), in *Proc. 1st Int. Symp. on Deformations in Turkey,* pp. 759–769, TMMOB-HKMO, Ankara.

Ambraseys, N.N. & Jackson, J.A., 1990. Seismicity and associated strain of central Greece between 1890 and 1988, *Geophys. J. Int.,* **101,** 663–708.

Ambraseys, N.N. & Jackson, J.A., 1997. Seismicity and strain in central Greece since 1694, *J. Earthq. Eng.,* **1,** 433–474.

Angelier, J., Lybéris, N., Le Pichon, X., Barrier, E. & Huchon, P., 1982. The tectonic development of the Hellenic arc and the Sea of Crete: a synthesis, *Tectonophys,* **86,** 159–196.

Argus, D.F. & Gordon, R.G., 1990. Pacific–North American plate motion from Very Long Baseline Interferometry compared with motion inferred from magnetic anomalies, transform faults, and earthquake slip vectors, *J. geophys. Res.,* **95**(B11), 17 315–17 324.

Argus, D.F. & Gordon, R.G., 1991. No-net-rotation model of current plate velocities incorporating plate motion model Nuvel-1, *Geophys. Res. Lett.,* **18**(11), 2039–2042.

Armijo, R., Meyer, B., King, G.C.P., Rigo, A. & Papanastassiou, D., 1996. Quaternary evolution of the Corinth Rift and its implications for the Late Cenozoic evolution of the Aegean, *Geophys. J. Int.,* **126,** 11–53.

Ashkenazi, V., Bingley, R.M., Whitmore, G.M. & Baker, T.F., 1993. Monitoring changes in mean sea-level to millimetres using GPS, *Geophys. Res. Lett.,* **20,** 1951–1954.

Bernard, P. *et al.,* 1997. The $M_s = 6.2$, June 15, 1995 Aigion earthquake (Greece): evidence for low angle normal faulting in the Corinth rift, *J. Seismol.,* **1,** 131–150.

Beutler, G., Brockmann, E., Gurtner, W., Hugentobler, U., Mervart, L., Rothacher, M. & Verdun, A., 1994. Extended orbit modelling techniques at the CODE processing center of the international GPS service for geodynamics (IGS): theory and initial results, *Man. Geod.,* **19,** 367–386.

Billiris, H. *et al.,* 1991. Geodetic determination of tectonic deformation in central Greece from 1900 to 1988, *Nature,* **350,** 124–129.

Blewitt, G., Heflin, M.B., Webb, F.H., Lindqwister, U.J. & Malla, R.P., 1992. Global coordinates with centimetre accuracy in the International Terrestrial Reference Frame using GPS, *Geophys. Res. Lett.,* **19,** 853–856.

Boucher, C., Altamimi, Z. & Duhem, L., 1993. ITRF 92 and its Associated Velocity Field, *IERS Technical Note,* **15,** Observatoire de Paris, Paris.

Boucher, C., Altamimi, Z. & Duhem, L., 1994. Results and Analysis of the ITRF93, *IERS Technical Note,* **18,** Observatoire de Paris, Paris.

Bourne, S.J., England, P.C. & Parsons, B., 1998. The motion of crustal blocks driven by flow of the lower lithosphere and implications for slip rates of continental strike-slip faults, *Nature,* **391,** 655–659.

Clarke, P.J. *et al.,* 1997. Geodetic estimate of seismic hazard in the Gulf of Korinthos, *Geophys. Res. Lett.,* **24,** 1303–1306.

Cross, P.A., 1990. Practical integration of GPS and classical control networks, in *Proc. XIX FIG Congress,* pp. 336–348, Helsinki.

Curtis, A., England, P. & Davies, R., 1997. Local and regional components of western Aegean deformation extracted from 100 years of geodetic displacement measurements, *Geophys. J. Int.,* **130,** 623–639.

Davies, R.R., 1996. Geodetic and morphometric studies of crustal strain and active faulting in southern and central Greece, *D. Phil. thesis,* University of Oxford, Oxford.

Davies, R.R., England, P.C., Parsons, B.E., Billiris, H., Paradissis, D. & Veis, G., 1997. Geodetic strain of Greece in the interval 1892–1992, *J. geophys. Res.,* **102**(B11), 24 571–24 588.

DeMets, C., Gordon, R.G., Argus, D.F. & Stein, S., 1994. The effect of recent revisions to the geomagnetic reversal time scale on estimates of current plate motions, *Geophys. Res. Lett.,* **21,** 2191–2194.

Denys, P.H. *et al.,* 1995. GPS networks for determining the accumulation of current crustal strain in central Greece, in *Proc. 1st Int. Symp. on Deformations in Turkey,* pp. 748–758, TMMOB-HKMO, Ankara.

Dewey, J. & Şengör, A.M.C., 1979. Aegean and surrounding regions: complex multiplate and continuum tectonics in a convergent zone, *Geol. Soc. Am. Bull.,* **90,** 84–92.

GJI000 14/9/98 12:33:59 3B2 version 5.20
The Charlesworth Group, Huddersfield 01484 517077

Doutsos, T. & Poulimenos, G., 1992. Geometry and kinematics of active faults and their seismotectonic significance in the western Corinth–Patras rift (Greece), *J. struct. Geol.,* **14,** 689–699.

Giardini, D., di Donato, M. & Boschi, E., 1997. Calibration of magnitude scales for earthquakes of the Mediterranean, *J. Seismol.,* **1,** 161–180.

Gilbert, L.E., Kastens, K., Hurst, K., Paradissis, D., Veis, G., Billiris, H., Höppe, W. & Schlüter, W., 1994. Strain results and tectonics from the Aegean GPS experiment, *EOS, Trans. Am. geophys. Un.,* **75,** 116.

Gutenerg, B. & Richter, C.F., 1954. *Seismicity of the Earth,* Princeton University Press, Princeton.

Jackson, J. & McKenzie, D., 1988a. Rates of active deformation in the Aegean Sea and surrounding regions, *Basin Res.,* **1,** 121–128.

Jackson, J. & McKenzie, D., 1988b. The relationship between plate motions and seismic moment tensors and the rate of active deformation in the Mediterranean and Middle East, *Geophys. J. R. astr. Soc.,* **93,** 45–73.

Jackson, J., Haines, J. & Holt, W., 1994. A comparison of satellite laser ranging and seismicity data in the Aegean region, *Geophys. Res. Lett.,* **21,** 2849–2852.

Jackson, J.A., Haines, J. & Holt, W., 1992. The horizontal velocity field in the deforming Aegean Sea region determined from the moment tensors of earthquakes, *J. geophys. Res.,* **97**(B12), 17 657–17 684.

Kahle, H.-G., Muller, M., Mueller, S. & Veis, G., 1993. The Kephalonia transform fault and the rotation of the Apulian platform: evidence from satellite geodesy, *Geophys. Res. Lett.,* **20,** 651–654.

Kahle, H.-G., Muller, M.V., Geiger, A., Danuser, G., Mueller, S., Veis, G., Billiris, H. & Paradissis, D., 1995. The strain field in northwestern Greece and the Ionian Islands: results inferred from GPS measurements, *Tectonophys,* **249,** 41–52.

Kahle, H.-G., Muller, M.V. & Veis, G., 1996. Trajectories of crustal deformation of western Greece from GPS observations 1989–1994, *Geophys. Res. Lett.,* **23,** 677–680.

Kastens, K.A. *et al.,* 1989. The Aegean GPS Project: 1988 results and 1989 plans, *EOS, Trans. Am. geophys. Un.,* **70,** 306.

King, G.C.P., Ouyang, Z.X., Papadimitriou, P., Deschamps, D., Gagnepain, J., Houseman, G., Jackson, J.A., Soufleris, C. & Virieux, J., 1985. The evolution of the Gulf of Corinth, Greece: an aftershock study of the 1981 earthquakes, *Geophys. J. R. astr. Soc.,* **80,** 677–693.

Kostrov, B., 1974. Seismic moment and energy of earthquakes, and seismic flow of rock, *Izv. Acad. Sci. USSR Phys. Solid Earth,* **97,** 23–44.

Le Pichon, X. & Angelier, J., 1979. The Hellenic arc and trench system a key to the neotectonic evolution of the eastern Mediterranean area, *Tectonophys,* **60,** 1–42.

Le Pichon, X. & Angelier, J., 1981. The Aegean Sea, *Phil. Trans. R. Soc. Lond.,* A, **300,** 357–372.

Le Pichon, X., Chamot-Rooke, N., Lallemant, S., Noomen, R. & Veis, G., 1995. Geodetic determination of the kinematics of central Greece with respect to Europe: implications for eastern Mediterranean tectonics, *J. geophys. Res.,* **100**(B7), 12 765–12 690.

McKenzie, D., 1972. Active tectonics of the Mediterranean region, *Geophys. J. R. astr. Soc.,* **30,** 109–185.

McKenzie, D., 1978. Active tectonics of the Alpine–Himalayan belt: the Aegean Sea and surrounding regions, *Geophys. J. R. astr. Soc.,* **55,** 217–254.

Noomen, R., Ambrosius, B.A.C. & Wakker, K.F., 1993. Crustal motions in the Mediterranean region determined from laser ranging to LAGEOS, in *Contributions of Space Geodesy to Geodynamics: Crustal Dynamics,* pp. 331–346, eds Smith, D.E. & Turcotte, D.L., *AGU Geodynamics Series,* Vol. 23, Washington.

Okada, Y., 1985. Surface deformation due to shear and tensile faults in a half-space, *Bull. seism. Soc. Am.,* **75,** 1135–1154.

Papazachos, B.C., 1990. Seismicity of the Aegean and surrounding area, *Tectonophysics,* **178,** 287–308.

Papazachos, B.C. & Papazachos, C.B., 1989. *The Earthquakes of Greece,* Ziti Publications, Thessaloniki (in Greek).

Press, W.H., Teukolsky, S.A., Vetterling, W.T. & Flannery, B.P., 1992. *Numerical Recipes in C: The Art of Scientific Computing,* 2nd edn, Cambridge University Press, Cambridge.

Rigo, A., Lyon-Caen, H., Armijo, R., Deschamps, A., Hatzfeld, D., Makropoulos, K., Papadimitriou, P. & Kassaras, I., 1996. A microseismic study in the Gulf of Corinth (Greece): implications for large-scale normal faulting mechanisms, *Geophys. J. Int.,* **126,** 663–688.

Robbins, J.W., Smith, D.E. & Ma, C., 1993. Horizontal crustal deformation and large-scale plate motions inferred from space geodetic techniques, in *Contributions of Space Geodesy to Geodynamics: Crustal Dynamics,* pp. 21–36, eds Smith, D.E. & Turcotte, D.L., *AGU Geodynamics Series,* Vol. 23, Washington.

Rothacher, M. & Mervart, L., 1996. *Bernese GPS Software Version 4.0,* Astronomical Institute, University of Berne.

Rothacher, M., Beutler, G., Gurtner, W., Brockmann, E. & Mervart, L., 1993. *Bernese GPS Software Version 3.4 Documentation,* Astronomical Institute, University of Berne.

Rundle, J.B., 1982. Viscoelastic-gravitational deformation by a rectangular thrust fault in a layered Earth, *J. geophys. Res.,* **87**(B9), 7787–7796.

Savage, J.C. & Burford, R., 1970. Accumulation of tectonic strain in California, *Bull. seism. Soc. Am.,* **60,** 1877–1896.

Smith, D.E., Kolenkiewicz, R., Robbins, J.W., Dunn, P.J. & Torrence, M.H., 1994. Horizontal crustal motion in the central and eastern Mediterranean inferred from Satellite Laser Ranging measurements, *Geophys. Res. Lett.,* **21,** 1979–1982.

Stewart, M.P., Ffoulkes-Jones, G.H., Ochieng, W.Y. & Shardlow, P.J., 1995. *GAS: GPS Analysis Software User Manual Version 2.3,* IESSG, University of Nottingham.

Taymaz, T., Jackson, J. & McKenzie, D., 1991. Active tectonics of the north and central Aegean Sea, *Geophys. J. Int.,* **106,** 433–490.

University of Newcastle upon Tyne, 1994. Measurement of crustal deformation in central Greece using GPS satellites, *Dept Surveying Technical Report,* **94/0411.**

GJI000 14/9/98 12:34:03 3B2 version 5.20
The Charlesworth Group, Huddersfield 01484 517077